

**Boore-Atkinson NGA Empirical Ground Motion
Model for the Average Horizontal
Component of PGA, PGV and
SA at Spectral Periods of
0.1, 0.2, 1, 2, and 3 Seconds**

Interim Report for USGS Review

**May 31, 2006
(Revised July 6, 2006)**

by

David M. Boore
U.S. Geological Survey
Menlo Park, California

and

Gail M. Atkinson
Carleton University
Ottawa, Ontario, Canada

Provisional Ground-Motion Prediction Equations

By

David M. Boore
Gail M. Atkinson

Date: 6 July 2006

File: ba_provisional_equations_december2005_v1.5.doc

Introduction

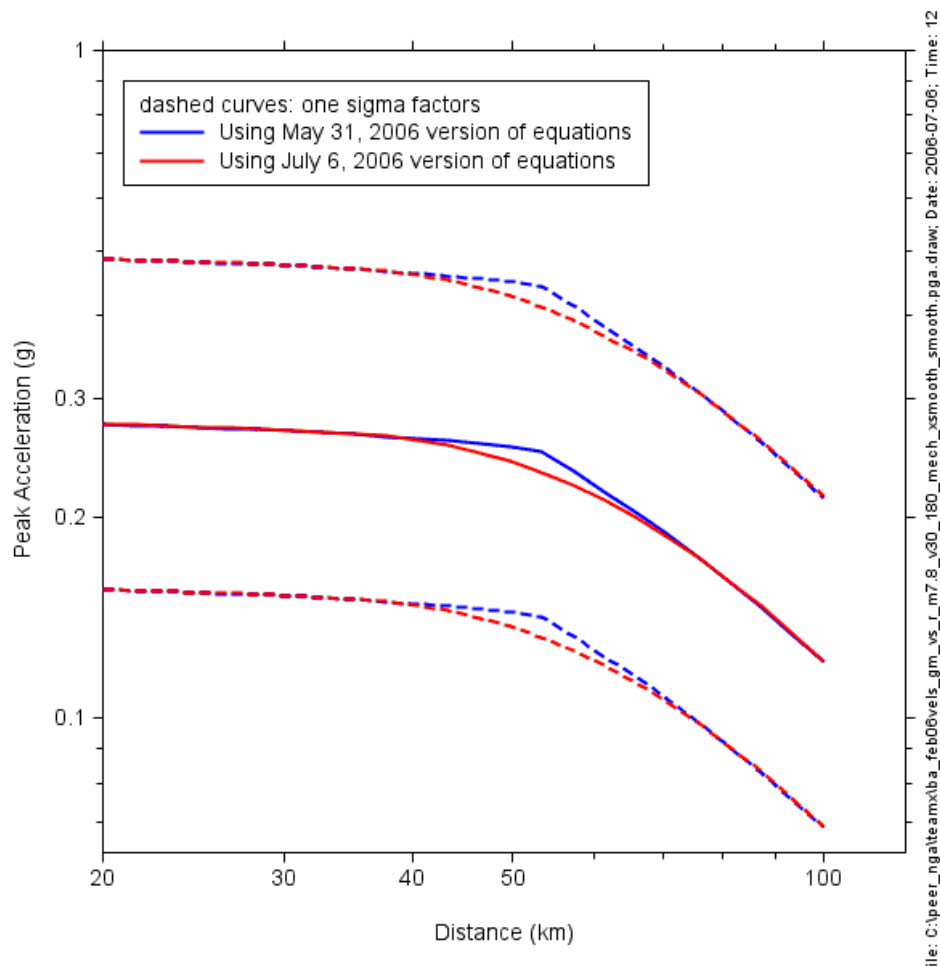
This report contains provisional empirically-based equations for predicting peak acceleration, peak velocity, and pseudo spectral acceleration at periods of 0.1, 0.2, 1, 2, and 3 seconds. This report builds on a report describing an earlier version of the equations, prepared in August 2005. That report, and accompanying files, are available from the online publications link on the first author's web site (<http://quake.usgs.gov/~boore/>).

Limited time was available to investigate the provisional equations. No residuals were plotted, but comparisons of the predicted motions were made against the distance and magnitude dependence of the data (the former for the smallest earthquake in the dataset and the ten earthquakes with magnitudes between 7.0 and 8.0). Among other things, many residual plots should be prepared, and the regressions should be repeated with randomly selected earthquakes and/or data removed from the dataset (in order to investigate the leverage of specific data on the results). For the form of the August equations, we repeated the regression excluding the 1999 Chi-Chi mainshock (no aftershock data were used in our regressions). The ground-motion predictions with and without the Chi-Chi mainshock were quite similar. We did not have time to redo that analysis for the revised equations in this report.

The functional form of the equations is given below, and the coefficients can be found in the Excel file

ba_rle400_c1_c2_fix_h_feb06vels_smooth_usnr.xls (the first row of coefficients in the file contains coefficients for *pga_{4nl}*).

This is a slight revision of the report issued by PEER on May 31, 2006. It includes a smoothed rather than abrupt transition for the nonlinear part of the amplification in the vicinity of *pga_{low}* (0.06g). The previous version could result in a kink in plots of ground motion vs. distance. The following figure shows an example using the May 31, 2006 and the current (smoothed) version of the equations). The computation was for a low shear-wave velocity, with the consequence that the deamplification due to nonlinear site response balances the increase in rock motions with decreasing distance within about 20 km:



Data Selection

During the course of the project, the first author spent a large amount of time on spot checking the database. His reports are available on request.

Data were excluded based on a number of criteria; each criterion was assigned a number in a column of containing flatfile record number and flag. Only data with flag = 0 were used in developing the empirical ground-motion prediction equations. The criteria and assignments for each record number are given in the two Excel files:

recnum_flag.xls
flag_definitions.xls

The ground-motion values are NOT geometric mean values, but rather are values that are not dependent on the particular orientation of the instruments used to record the horizontal motion (in which case the geometric mean can be 0.0 if the motion were perfectly polarized along one

component direction). The measure used is discussed in the paper by Boore et al. (2006).

In this report equations are given for pgv , pga , and psa at 0.1, 0.2, 1.0, 2.0, and 3.0 sec.

Explanatory Variables

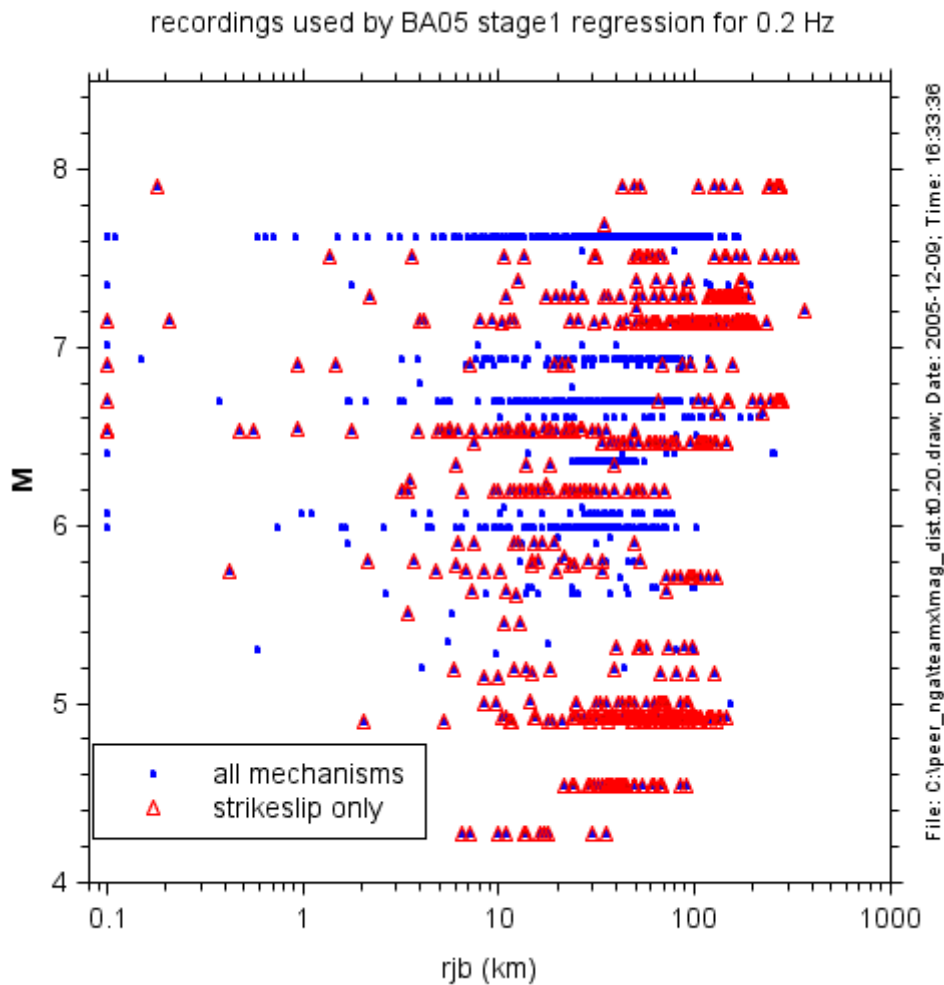
The magnitude is moment magnitude M , the distance is r_b distance, continuous V_{30} was used for site characterization (as given in the last column of the file **NGA Flatfile_nonPublic_V7.27.xls** by the combination of Silva's interpretation of NCREE measurements for Taiwan, Brian Chiou's correlation method for Taiwan, etc., updated with the file Update 1 (02-17-06) to NGA Flatfile V7.2 (07-11-05).xls, which uses some of Rob Kayen's V30 estimates). The mechanism was specified by the plunge of the P- and T-axes, as detailed in **fault_classification_using_p_t_axes.pdf** and **daves_notes_mechrake_c3_stage1_stage2_pga_25july2005.doc** (available from the first author upon request).

The analysis used the distances estimated by R. Youngs for earthquakes with no finite-fault models.

Methodology

Following the philosophy of Boore et al. (1993, 1994, 1997), simple equations were sought in the analysis. The analysis, however, is not purely based on the empirical analysis of the dataset. In particular, the soil amplifications were taken from Choi and Stewart (2005) for both linear and nonlinear amplifications (with a slight modification of the latter).

The analysis used the two-stage regression discussed by Joyner and Boore (1993, 1994). All regressions were done period-by-period; there was no smoothing of coefficients. The distance dependence is determined in the first stage. In the August version of the equations, a good fit to the distance decay was obtained using a single effective geometrical-spreading term---what is termed here the " c_1 " coefficient. (Note the increasing sparseness of data beyond about 80 to 100 km, as seen in the figure below).

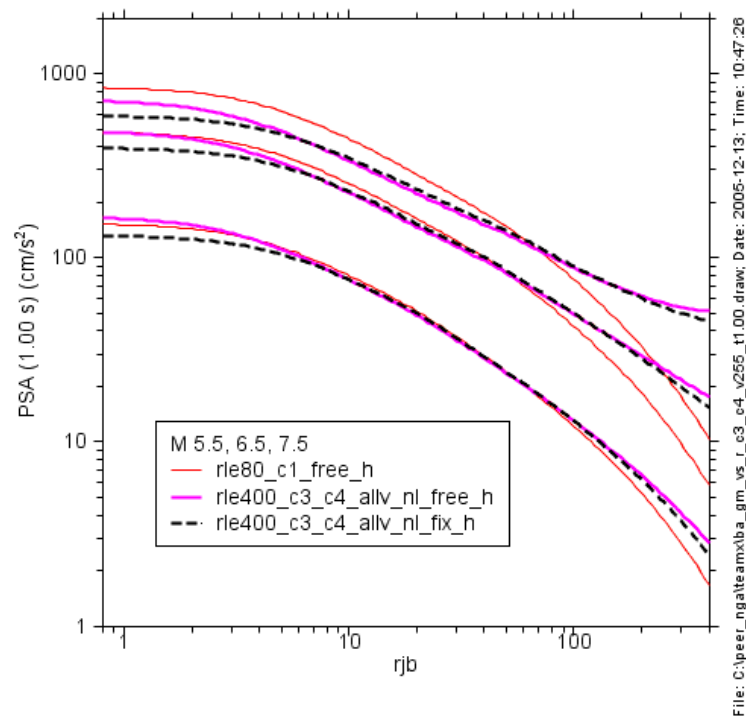


But because the data from several earthquakes underrepresented in the database clearly show a curvature (in log-log space), we did a separate analysis of a more complete dataset for three small events (compiled by J. Boatwright and L. Seekins) and for the 2004 Parkfield earthquake. The effective anelastic coefficient c_3 obtained from this analysis was then used in the regression of the NGA dataset for the August 2005 version of the equations. (Attempts to let both c_1 and c_3 be free resulted in positive values of c_3 for some periods, and this would lead to an increase of ground motion for great enough distances). For the August set of equations, after experimenting with various constraints, values of c_3 were fixed in the regression of the NGA dataset, with only the c_1 coefficient, pseudodepth h , and event terms as free variables ("event terms" is shorthand for the arithmetic average of the logarithm of the observations, corrected to a reference velocity of 760 m/s using the equation given later for F_s , adjusted to a distance of 5 km). The NGA data were first adjusted for linear and

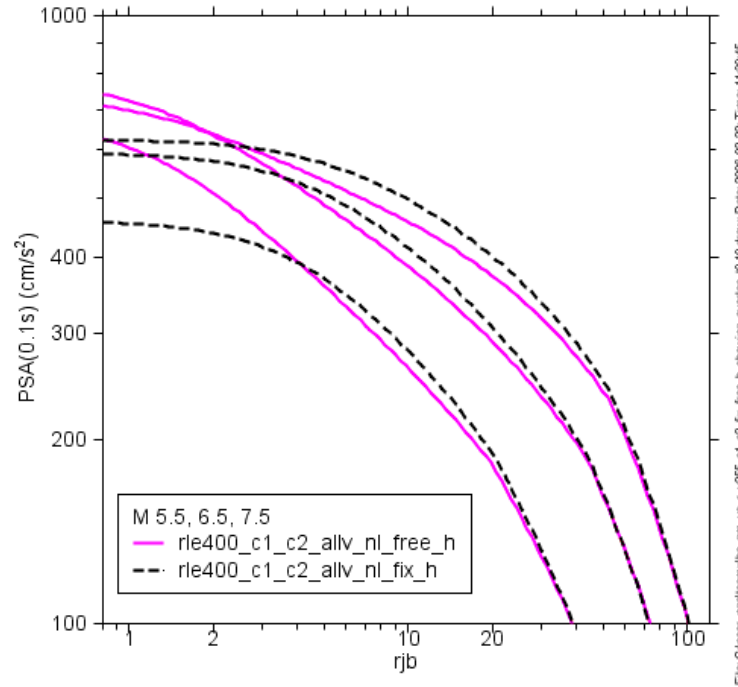
nonlinear site amplification to a V_{30} value of 760 m/s, using F_s below. Only data for $r_{jb} \leq 80$ km were used in the regression for the August equations, but all values of V_{30} were considered.

The equations given in the August report were developed using data only within 80 km, with the assumption that the distance dependence was independent of magnitude. Residual plots, as well as plot of motions from individual large earthquakes, showed a consistent mismatch between data and predictions for distances beyond 50 to 80 km. A number of ground-motion simulations supported this observation.

To add magnitude dependence, we used all data less than 400 km and tried letting the c_4 coefficient be a regression variable. The resulting equations, however, showed a tendency for increasing motions with distance (for large distances), for longer periods, as shown in this figure:

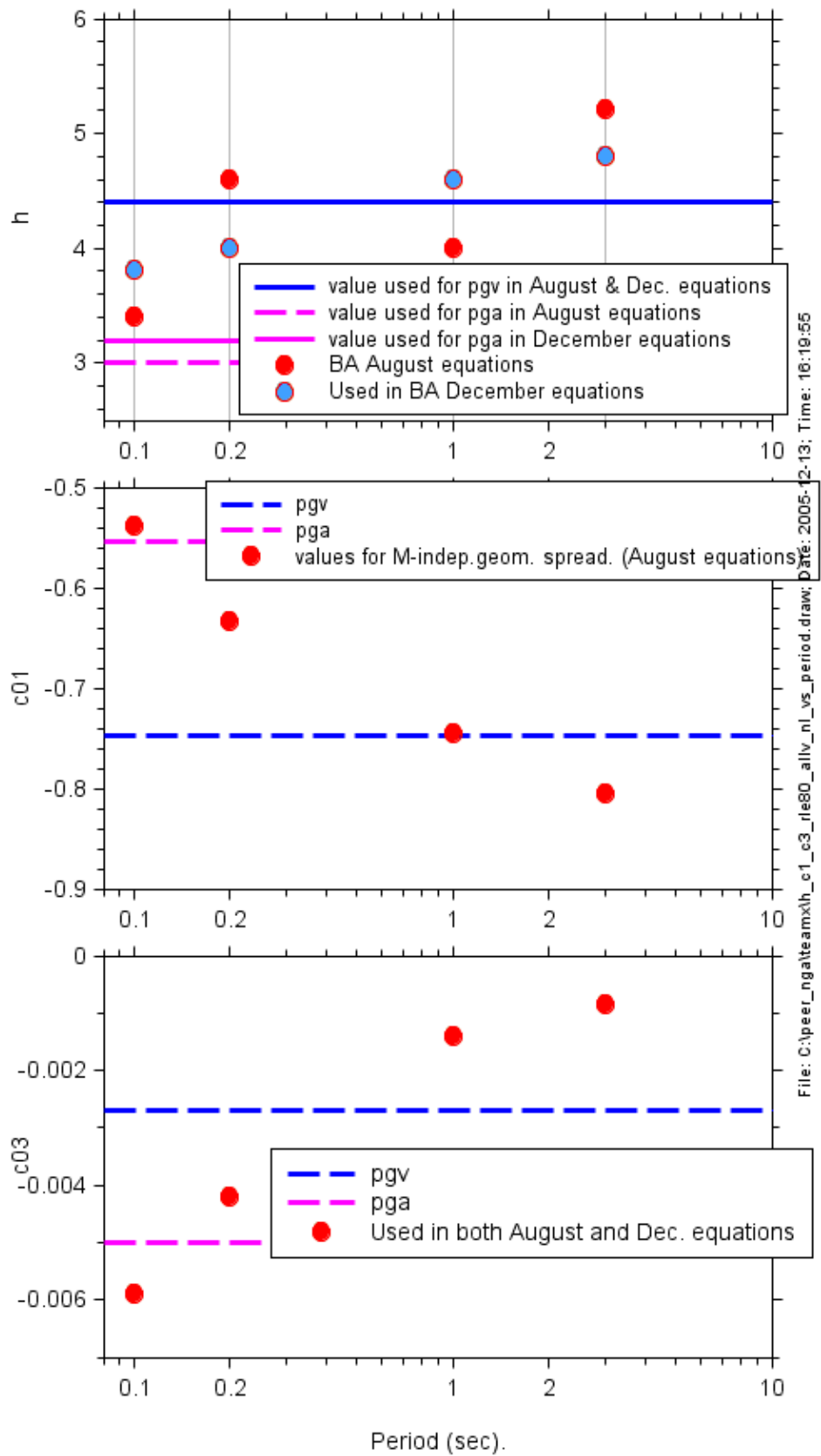


We then tried letting the coefficient c_2 be free. When we also let the pseudodepth h be free, we found that the curves for large earthquakes showed some overlap at close distances, as shown here:



The final set of provisional equations were determined by fixing the pseudodepth h at slightly smoothed versions of those given in the August report, with only c_1 and c_2 as free regression coefficients for the stage1 regression (in addition to event terms, which are basically the average ground motions for a single event projected to a distance of r_{ref}). The graph below shows values of h , c_1 , and c_3 . (Note that Bommer and Alarcón (2005) find that the pseudovelocity response spectrum at 0.5 sec is roughly equivalent to pgv ; pseudoacceleration response is equivalent to pga at periods much less than 0.1 sec).

Consideration was given to the amount of change at various distances when data only to 80 km was used, compared to using data to 400 km. See Choice of RLE400 or RLE80 equations.pdf for a discussion and relevant plots.



The event terms from the first regression were used in a weighted stage2 regression. As discussed in Joyner and Boore (1993), the stage2 regression was iterative in order to solve for σ_2 . Only events with more than one observation were used in the regression. The following algorithm was used for the magnitude dependence:

1. Do a single quadratic fit. If the M for which the quadratic starts to decrease (M_{\max}) is greater than 8.5, use this regression for the magnitude dependence.
2. If M_{\max} is less than 8.5, then do a two-segment regression, hinged at M_h , with a quadratic for $M \leq M_h$ and a linear function for $M_h < M$. If the slope of the linear function is positive, use this regression for the magnitude dependence.
3. If the slope of the linear segment is negative, redo the regression constraining the slope of the line above M_h to be 0.0.

The magnitude dependence was first done grouping all mechanisms. Plots of event terms vs. magnitude showed that normal fault earthquakes had motions consistently below those for strikeslip and reverse for most periods. For this reason, another set of equations was developed in which the magnitude dependence was constrained by the run using unspecified mechanism, with only the intercept term (the value for $M = M_{ref}$) as a free parameter.

All analyses were done using Fortran programs developed by DMB; these programs are available on request.

The Equations

The equation for predicting ground motions is:

$$\ln Y = F_M(M) + F_D(r_{jb}, M) + F_S(V_{30}, r_{jb}, M) + \varepsilon\sigma_{TU} + \varepsilon\sigma_{TM}$$

where σ_{TU} and σ_{TM} equal 1, 0 and 0,1 for mechanism unspecified and mechanism specified, respectively. The magnitude scaling is given by these equations:

For $M \leq M_h$

$$F_M(M) = e_1U + e_2S + e_3N + e_4R + e_5(M - M_h) + e_6(M - M_h)^2$$

For $M > M_h$

$$F_M(M) = e_1 U + e_2 S + e_3 N + e_4 R + e_7 (M - M_h) + e_8 (M - M_h)^2$$

where U , S , N , and R are used to specify the mechanism, as given by the values in the following table:

| Mechanism | U | S | N | R |
|-------------|---|---|---|---|
| unspecified | 1 | 0 | 0 | 0 |
| strikeslip | 0 | 1 | 0 | 0 |
| normal | 0 | 0 | 1 | 0 |
| reverse | 0 | 0 | 0 | 1 |

The distance scaling is given by

$$F_D(r_{jb}, M) = [c_1 + c_2 (M - M_{ref})] \ln(r / r_{ref}) + [c_3 + c_4 (M - M_{ref})] (r - r_{ref})$$

where

$$r = \sqrt{r_{jb}^2 + h^2}$$

The site amplification in the Dec. 05 equations (May 31, 2006) is given by these equations:

For $pga_{4nl} \leq pga_low$:

$$F_S(V_{30}, M, r_{jb}) = b_{lin} \ln(V_{30} / V_{ref}) + b_{nl} \ln(pga_low / 0.1)$$

For $pga_{4nl} > pga_low$:

$$F_S(V_{30}, M, r_{jb}) = b_{lin} \ln(V_{30} / V_{ref}) + b_{nl} \ln(pga_{4nl} / 0.1)$$

where the nonlinear factor is controlled by the slope b_{nl} , as given by the following equations (see May 31 PEER report). In the May 31 report, $pga_low = 0.06g$.

Let the linear and nonlinear terms be denoted by F_{LIN} and F_{NL} , so that

$$F_S = F_{LIN} + F_{NL}$$

where

$$F_{LIN} = b_{lin} \ln(V_{30} / V_{ref})$$

For $pga_{4nl} \leq pga_low$:

$$F_{NL} = b_{nl} \ln(pga_low / 0.1)$$

For $pga4nl > pga_low$:

$$F_{NL} = b_{nl} \ln(pga4nl / 0.1)$$

Note that $F_{NL} = 0.0$ for $pga4nl = 0.1$, because Choi and Stewart point out that the “linear” amps were derived for motions with about this mean (median?) amplitude.

But the discontinuous derivative of F_s with respect to $\ln(pga4nl / 0.1)$ at the hinge pga of pga_low leads to a kink in plots of ground motion vs distance (as shown in an earlier plot). A way around this is to use a cubic polynomial

$$F_{NL} = b_{nl} \ln(pga_low / 0.1) + b \ln(pga4nl / a_1) + c[\ln(pga4nl / a_1)]^2 + d[\ln(pga4nl / a_1)]^3$$

between $pga4nl = a_1$ and $pga4nl = a_2$ (on either side of pga_low). The coefficients can be found using the constraints that the polynomial and its slope must equal F_{NL} and its slope when $pga4nl = a_1$ and when $pga4nl = a_2$. These constraints lead to the following equations for the cubic coefficients b , c , and d :

$$b = 0.0$$

$$c = (3\Delta y - b_{nl}\Delta x) / \Delta x^2$$

$$d = -(2\Delta y - b_{nl}\Delta x) / \Delta x^3$$

where

$$\Delta x = \ln(a_2 / a_1)$$

and

$$\Delta y = b_{nl} \ln(a_2 / pga_low)$$

To summarize:

for $pga4nl \leq a_1$:

$$F_{NL} = b_{nl} \ln(pga_low / 0.1)$$

for $a_1 < pga4nl \leq a_2$:

$$F_{NL} = b_{nl} \ln(pga_low / 0.1) + c[\ln(pga4nl / a_1)]^2 + d[\ln(pga4nl / a_1)]^3$$

for $a_2 < pga4nl$:

$$F_{NL} = b_{nl} \ln(pga4nl / 0.1)$$

The nonlinear factor is controlled by the slope b_{nl} , as given by the following equations:

For $V_{30} \leq v_1$

$$b_{nl} = b_1$$

For $v_1 < V_{30} \leq v_2$

$$b_{nl} = (b_1 - b_2) \ln(V_{30} / v_2) / \ln(v_1 / v_2) + b_2$$

For $v_2 < V_{30} \leq v_{ref}$

$$b_{nl} = b_2 \ln(V_{30} / v_{ref}) / \ln(v_2 / v_{ref})$$

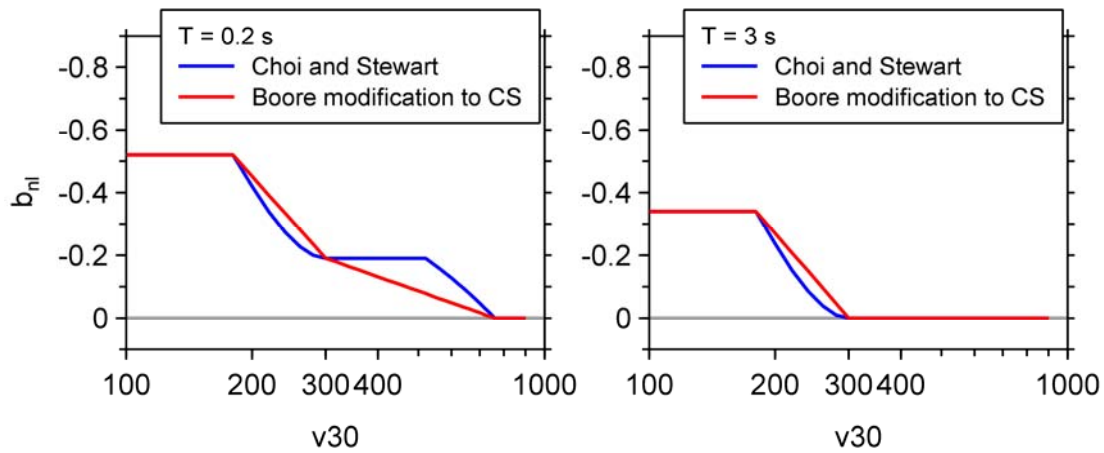
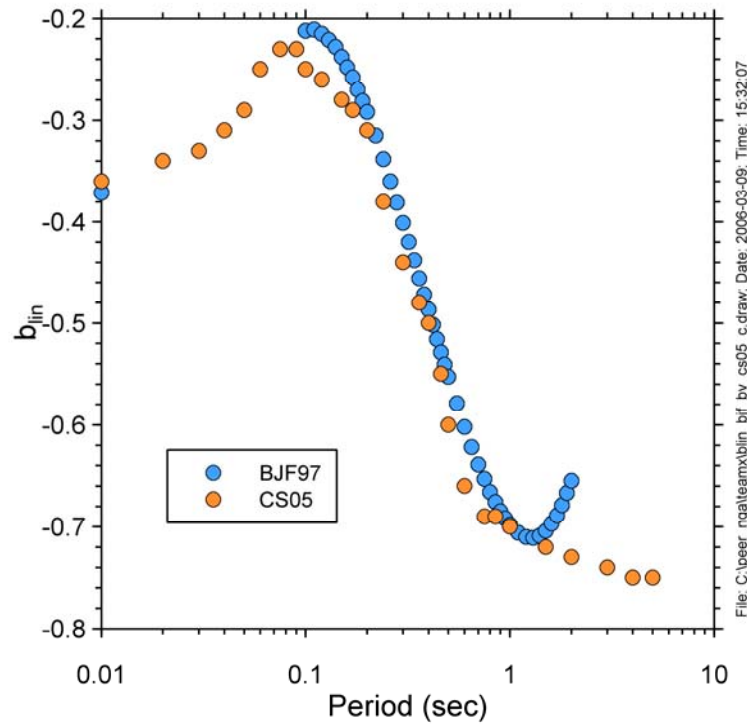
For $v_{ref} < V_{30}$

$$b_{nl} = 0.0$$

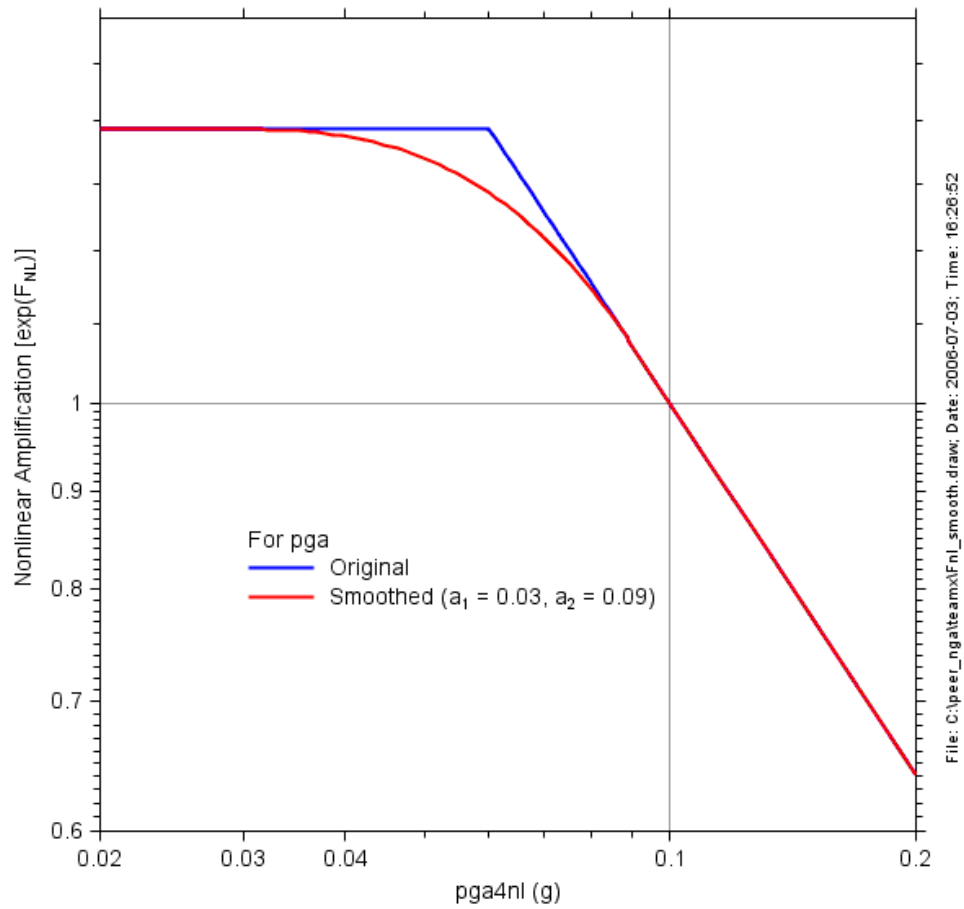
and $pga4nl$ is given by the equation for $\ln Y$ above, but with coefficients that will differ somewhat from the coefficients for $Y = pga$ (the coefficients for $pga4nl$ were developed earlier; they need only give approximately correct values for the peak acceleration on rock-like sites, as long as internal consistency is maintained---as is the case here, with the site amplifications being used to reduce the observations to a reference velocity before doing the regressions, and the same site amplifications being used when predicting ground motions using the results of the regressions). The coefficients for $pga4nl$ are in the first row of coefficients in

ba_rle400_c1_c2_fix_h_feb06vels_smooth_usnr.xls. More discussion of the nonlinear and linear corrections is contained in **daves_notes_on_including_nonlinear_amps_26july2005.doc** and **daves_notes_comparing_teamx_bjf_14augustjuly2005.doc**, available upon request.

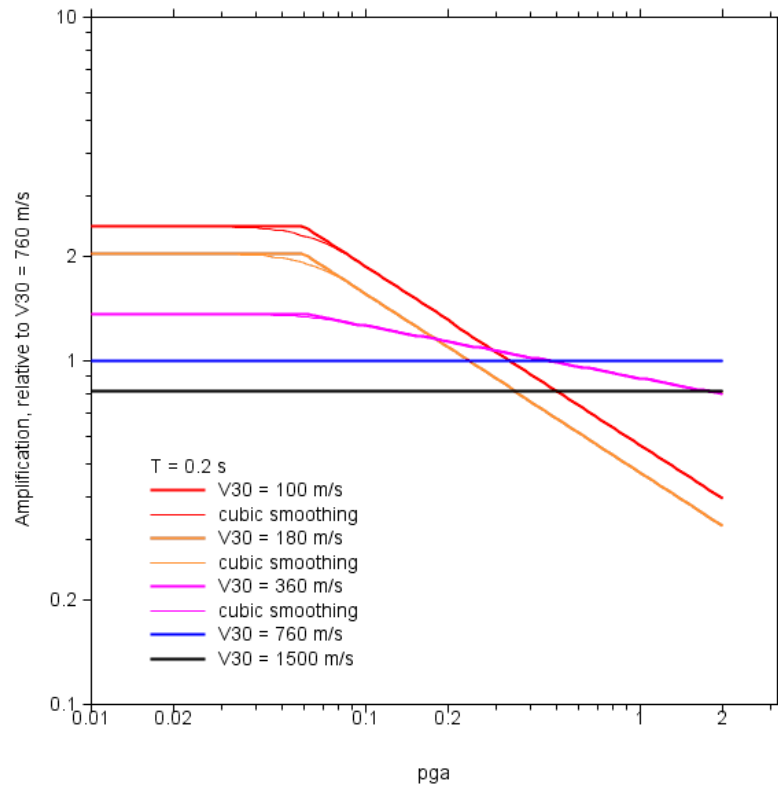
Here are plots of b_{lin} and b_{nl} :



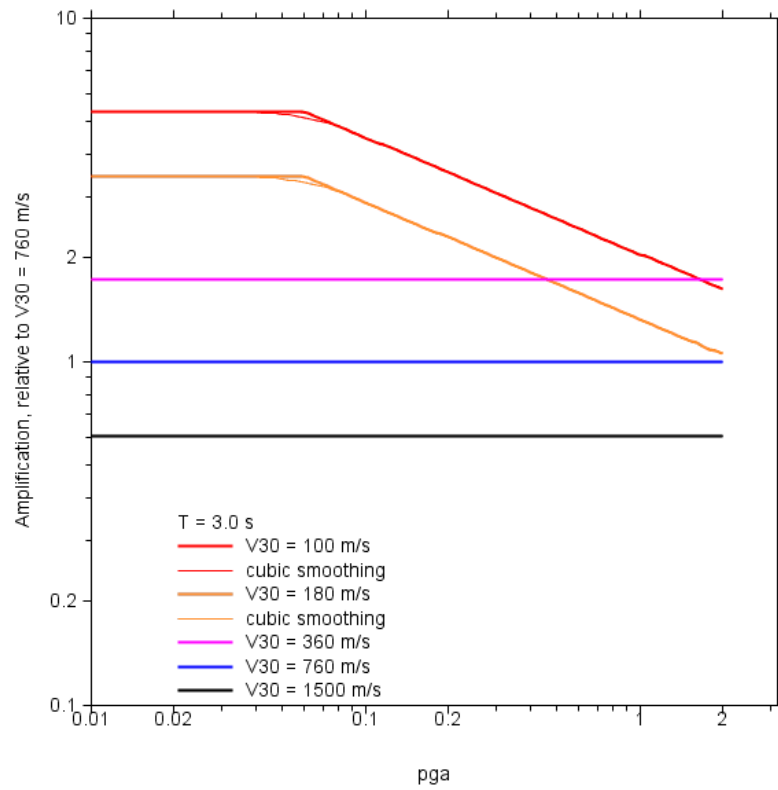
Here is a plot of the nonlinear contribution to site amplification showing how the cubic polynomial gives a smoothed version of the original amplification. The amplification is for $V_{30} = 180$ m/s:



And here are plots of the combined amplification for $T = 0.2s$ and $T = 3.0s$, with and without smoothing:



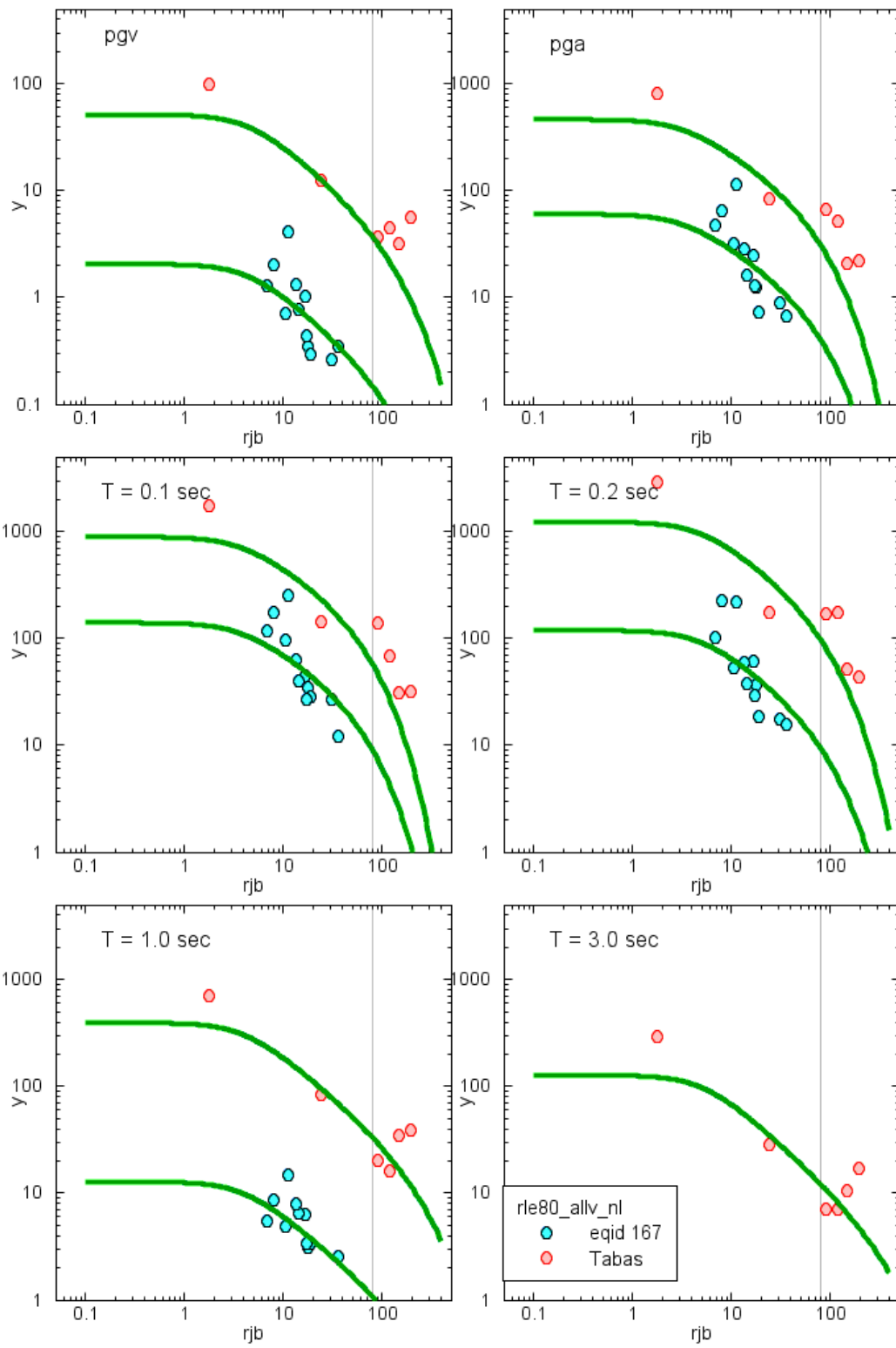
File: C:\peel_n\galteam\check_amp_n\1_dmb1_wd2.draw; Date: 2006-07-03; Time: 18:18:16



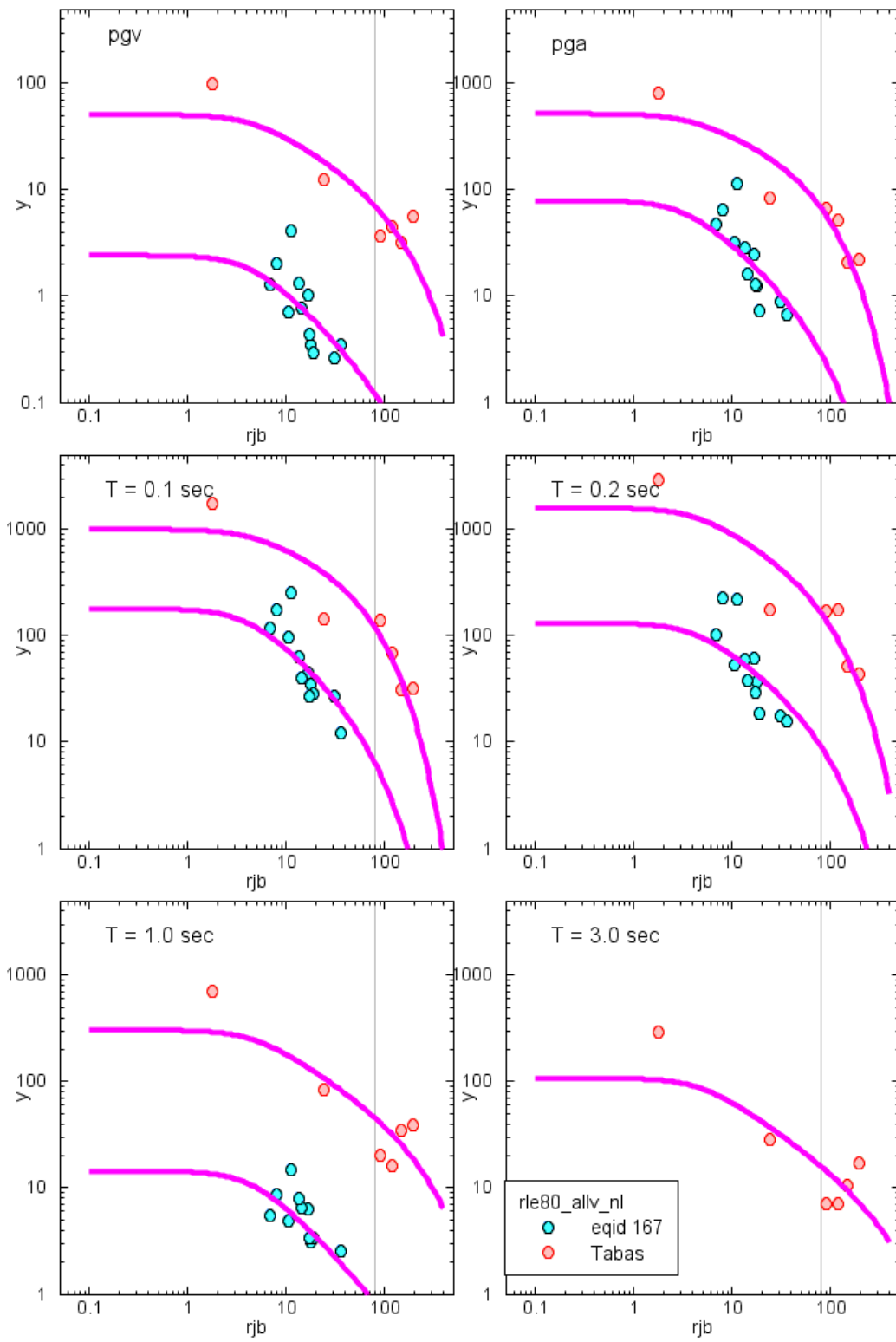
File: C:\peel_n\galteam\check_amp_n\1_dmb1_wd2.draw; Date: 2006-07-03; Time: 18:15:52

Comparison with Data

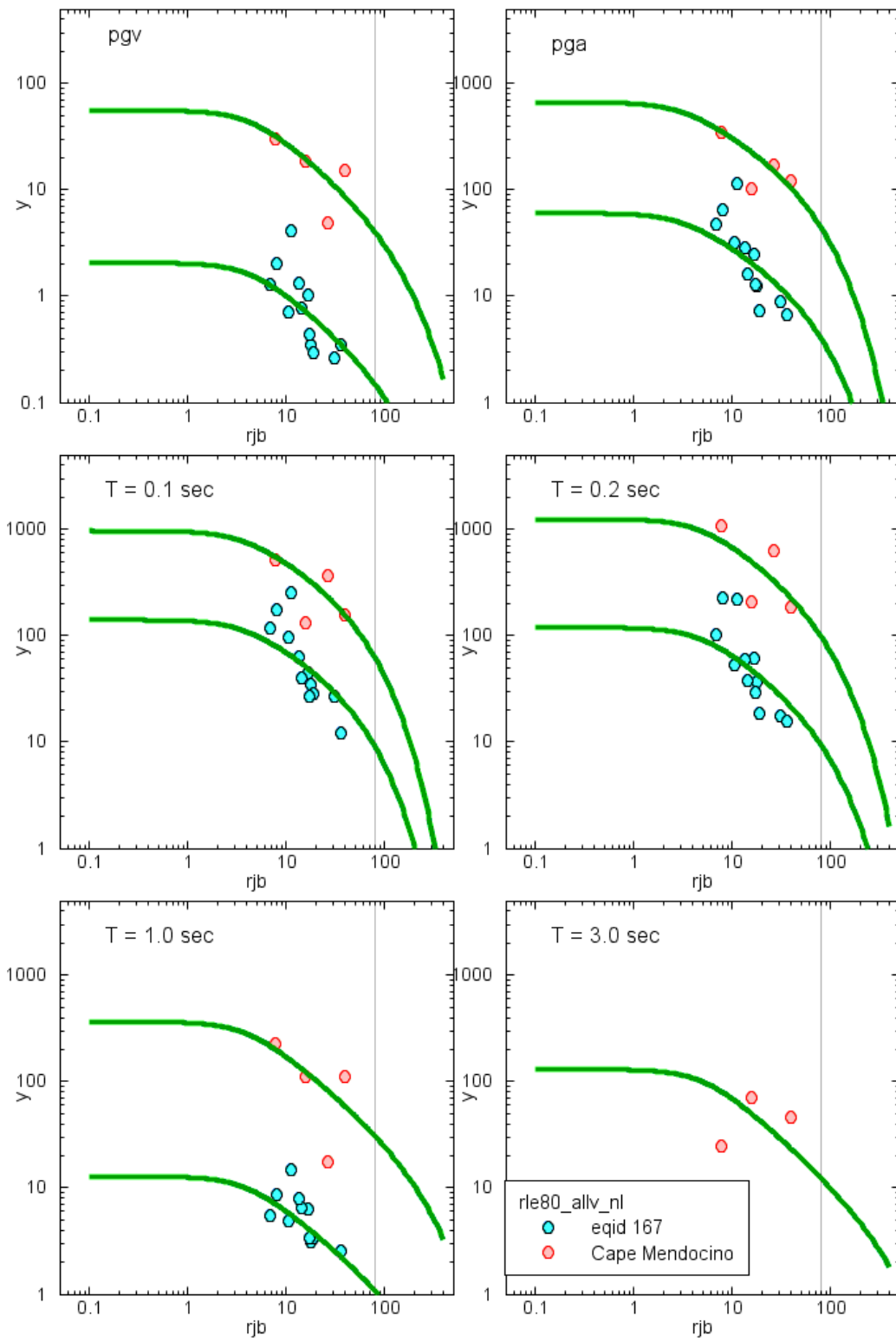
Inserted below are plots of ground motions vs. distance for the smallest earthquake (for comparison) and an earthquake with magnitude between 7 and 8 (see legend for specification of earthquake). The curves are from the regression fits and include the event terms found for the specific regression. The plots for the ten earthquakes are in pairs, the first plot of a pair corresponding to the magnitude-independent regression (basically, the August equations, except that the dataset changed slightly) and the second plot of a pair corresponding to the equations in this report.



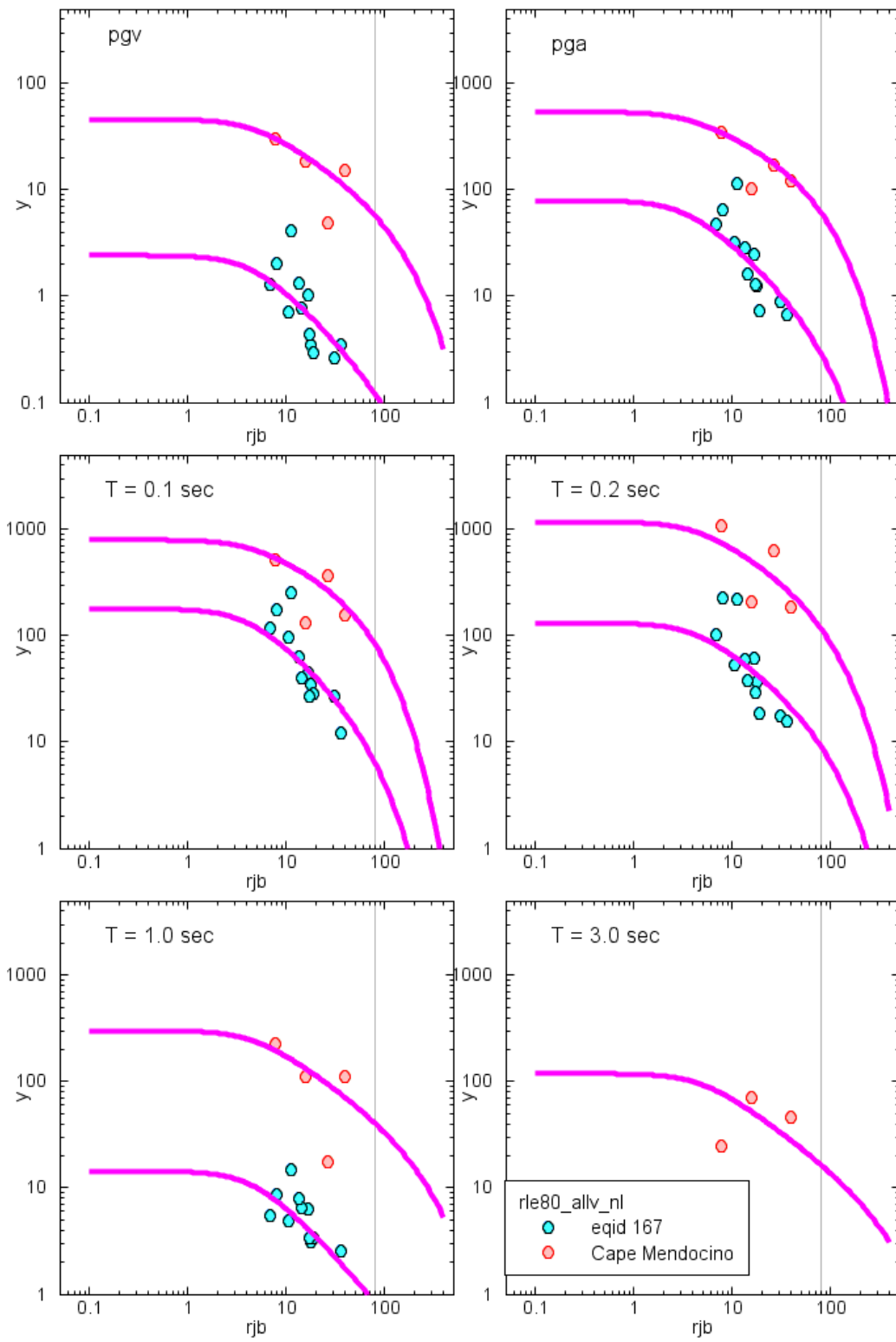
File: C:\peer_ngatteam\stage1_gm_rle80_allv_nl_eqid_167.draw; Date: 2006-12-12; Time: 15:37:01



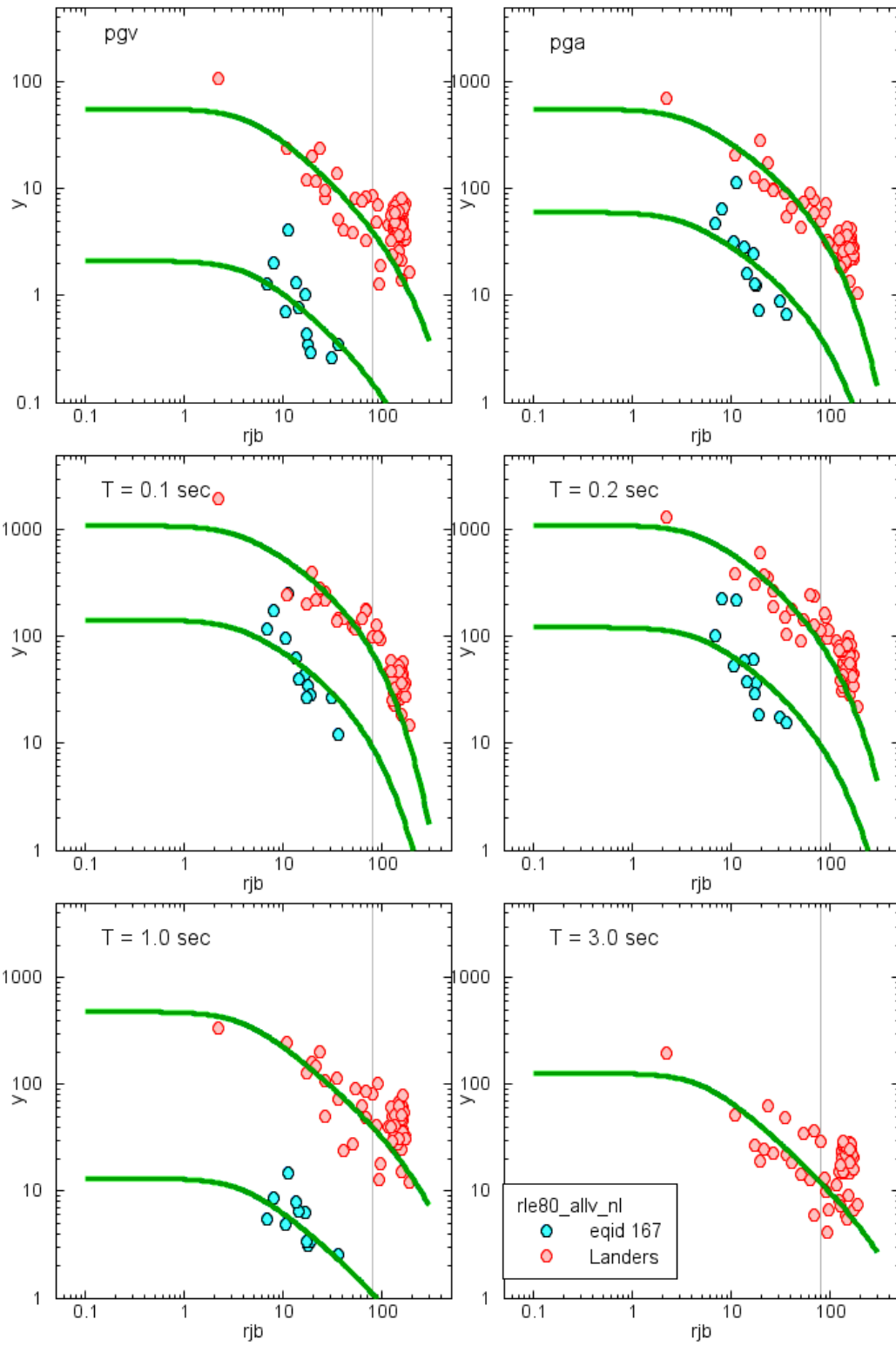
File: C:\peer_ngatteam\stage1_gm_rle400_e1_e2_fix_h_allv_nl_eqid_046_167.draw; Date: 2005-12-12; Time: 17:35:49



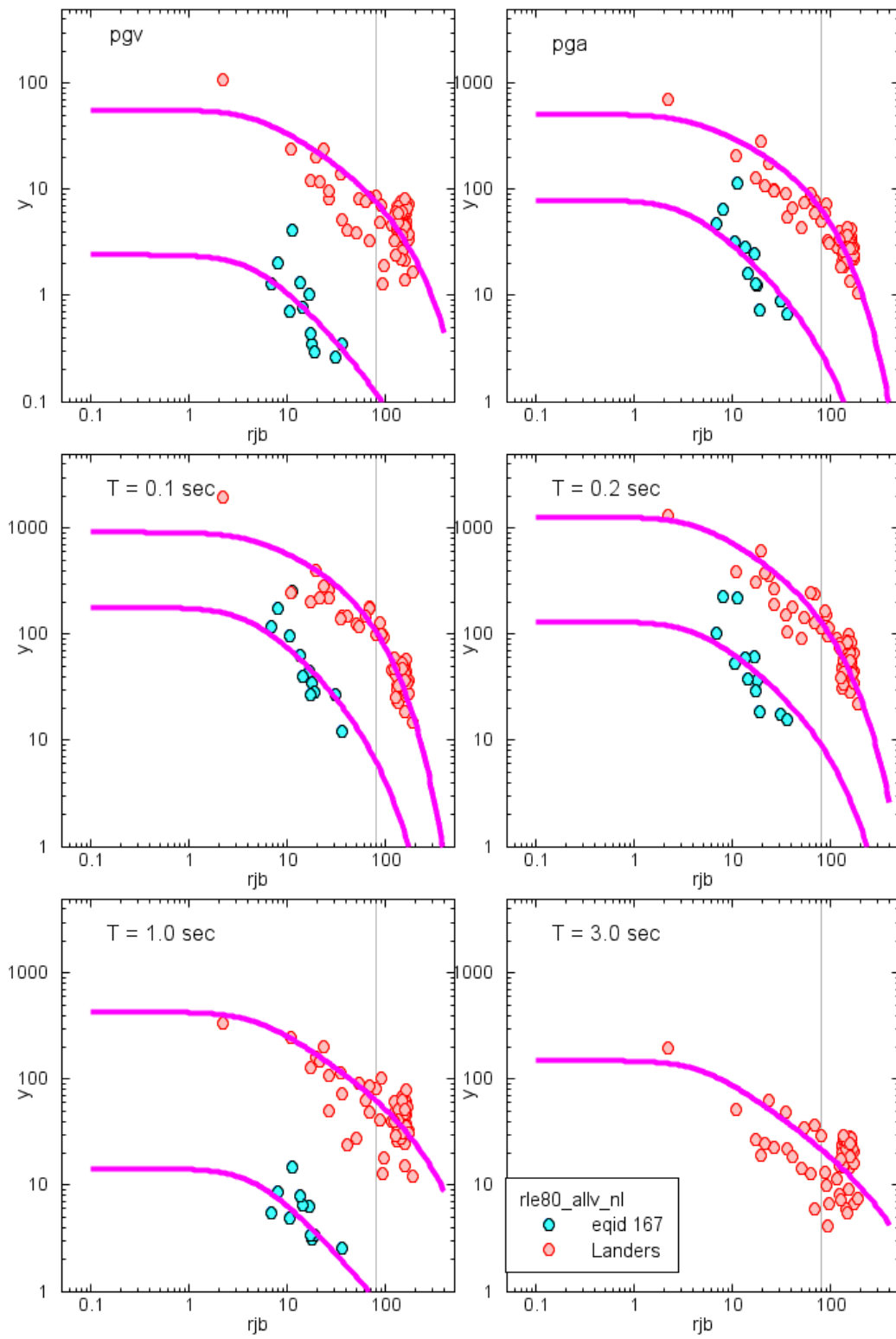
File: C:\peer_ngatteam\stage1_gm_rle80_allv_nl_eqid_123_167.draw; Date: 2006-12-12; Time: 15:37:31



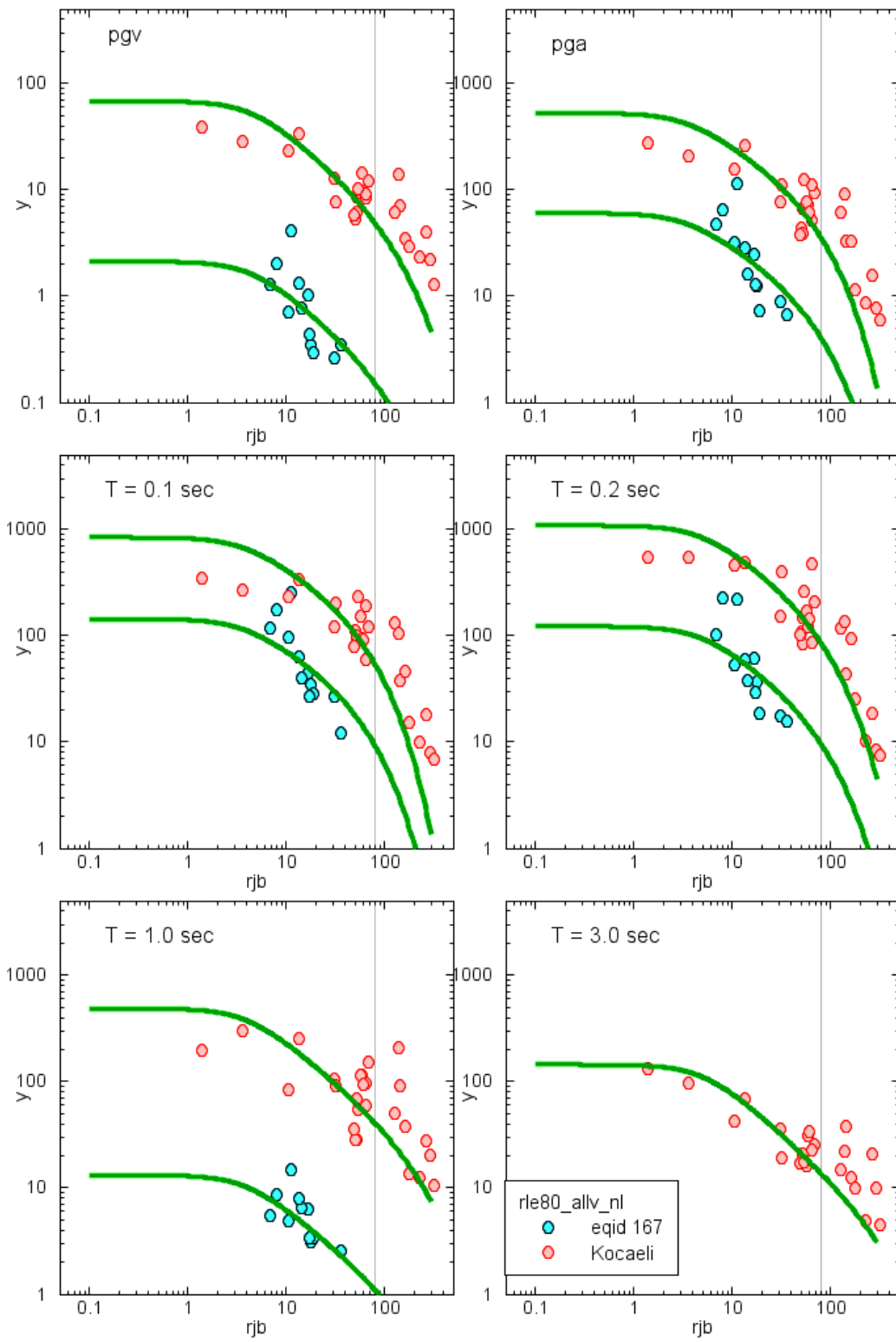
File: C:\peer_ngeteam\stage1_gm_rle400_e1_e2_fix_h_allv_nl_eqid_123_167.draw; Date: 2005-12-12; Time: 17:41:34



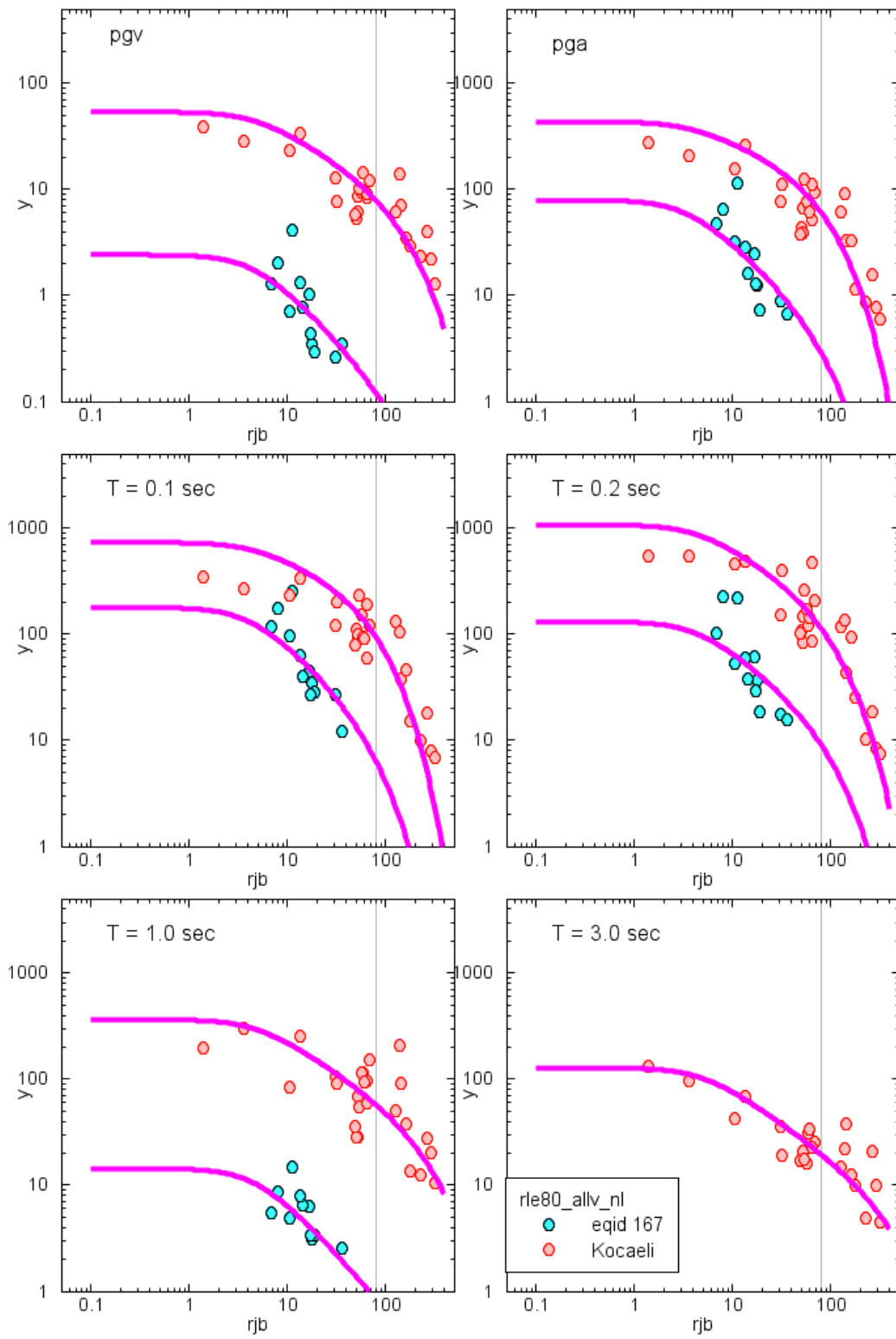
File: C:\peer_ngatteam\stage1_gm_rle80_allv_nl_eqid_125_167.draw; Date: 2006-12-07; Time: 10:39:41



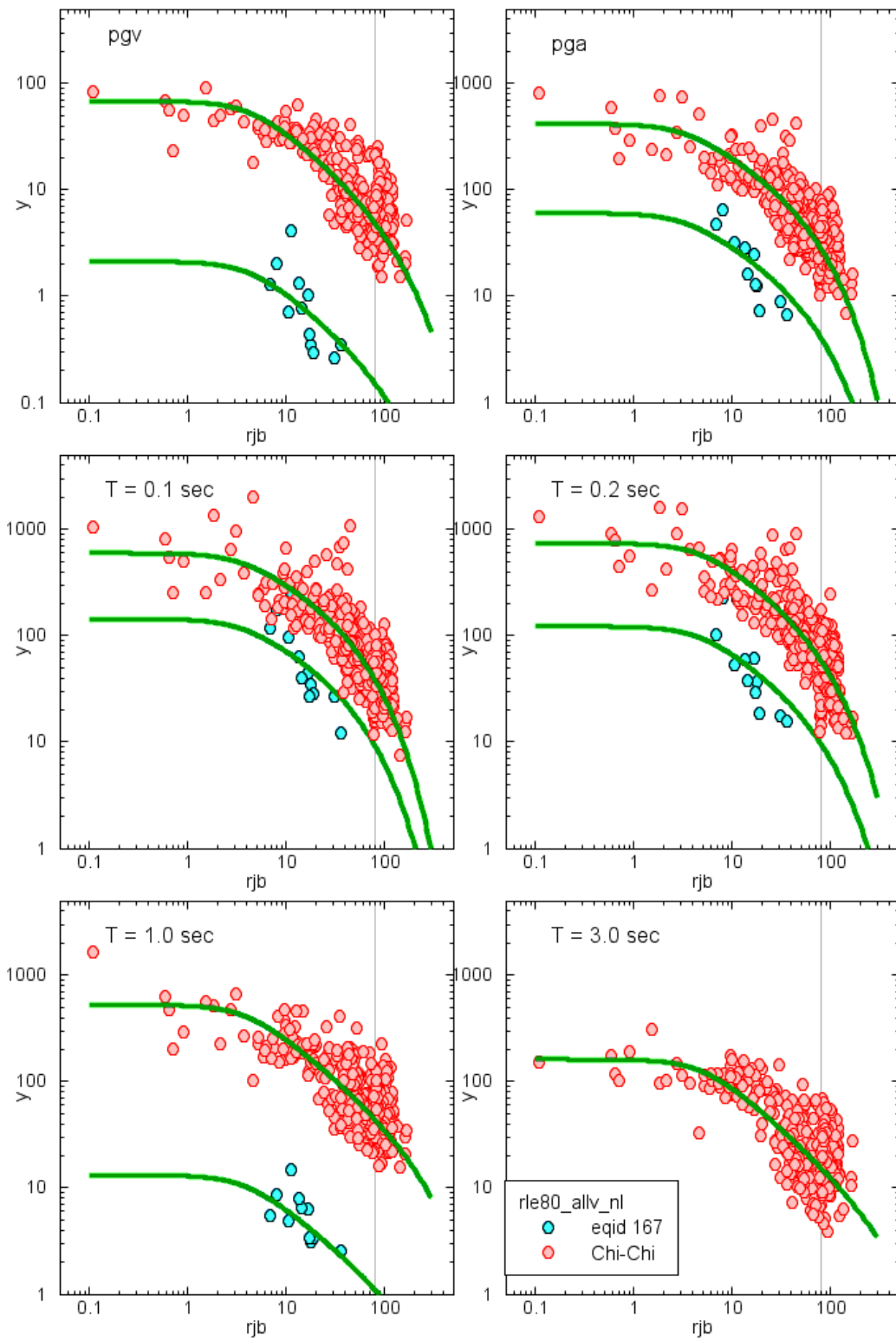
File: C:\peer_ngeteam\stage1_gm_tle400_e1_e2_fix_h_allv_nl_eqid_125_167.draw; Date: 2005-12-12; Time: 17:42:13



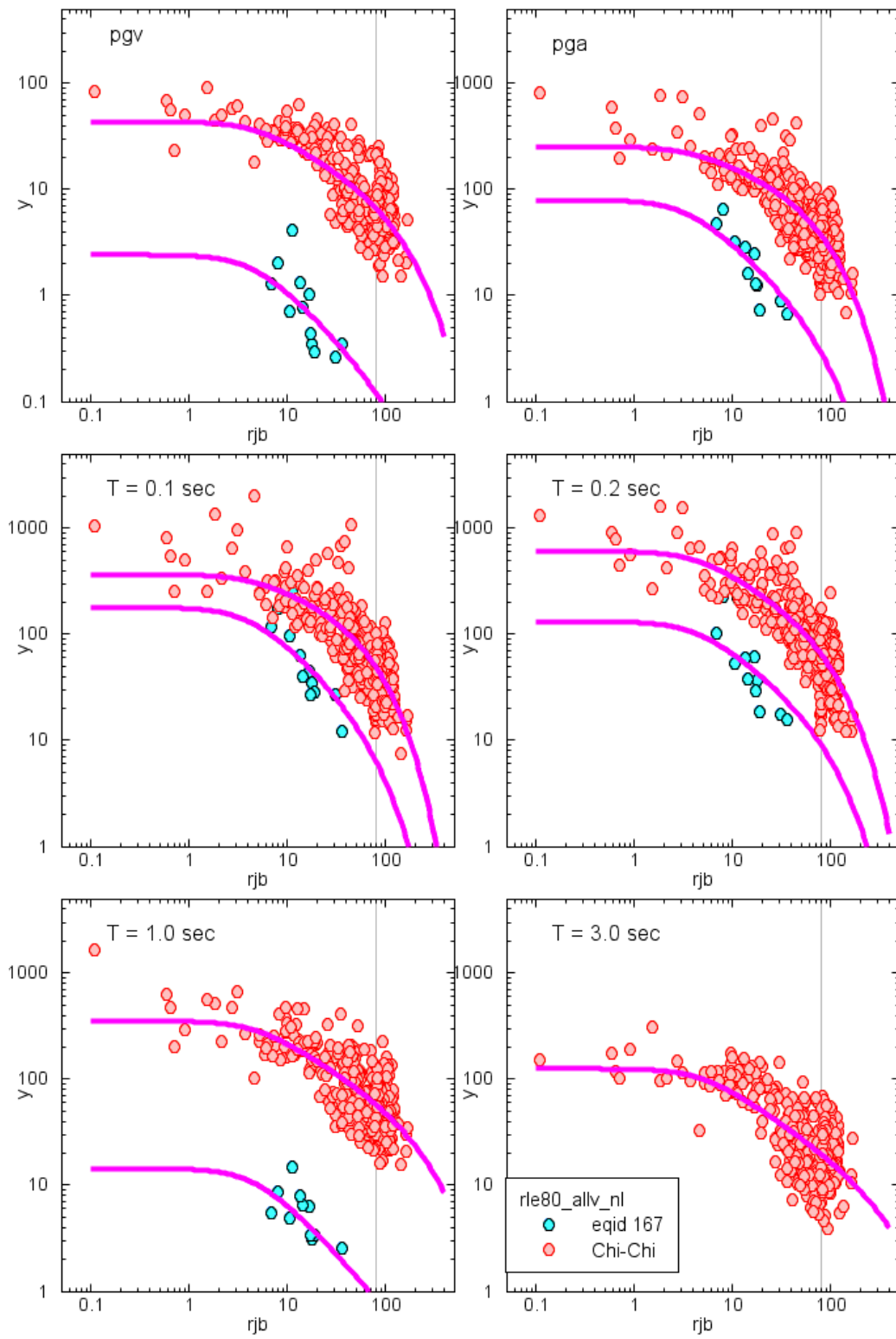
File: C:\peel_ngatteam\stage1_gm_rle80_allv_nl_eqid_136_167.draw; Date: 2005-12-07; Time: 19:57:08



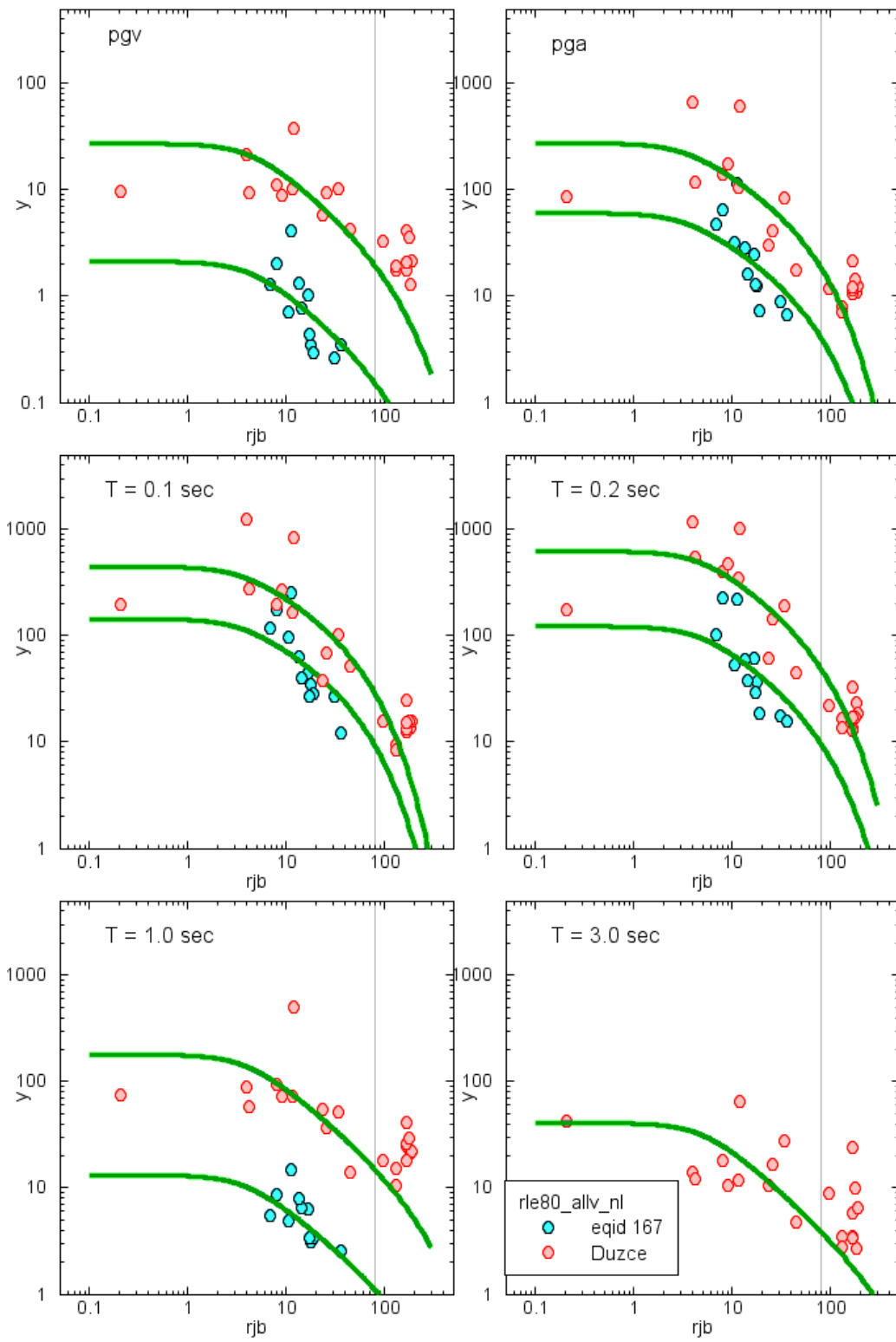
File: C:\peer_ngateam\stage1_gm_tle400_e1_e2_fix_h_allv_ni_eqid_136_167.draw; Date: 2005-12-12; Time: 17:43:25



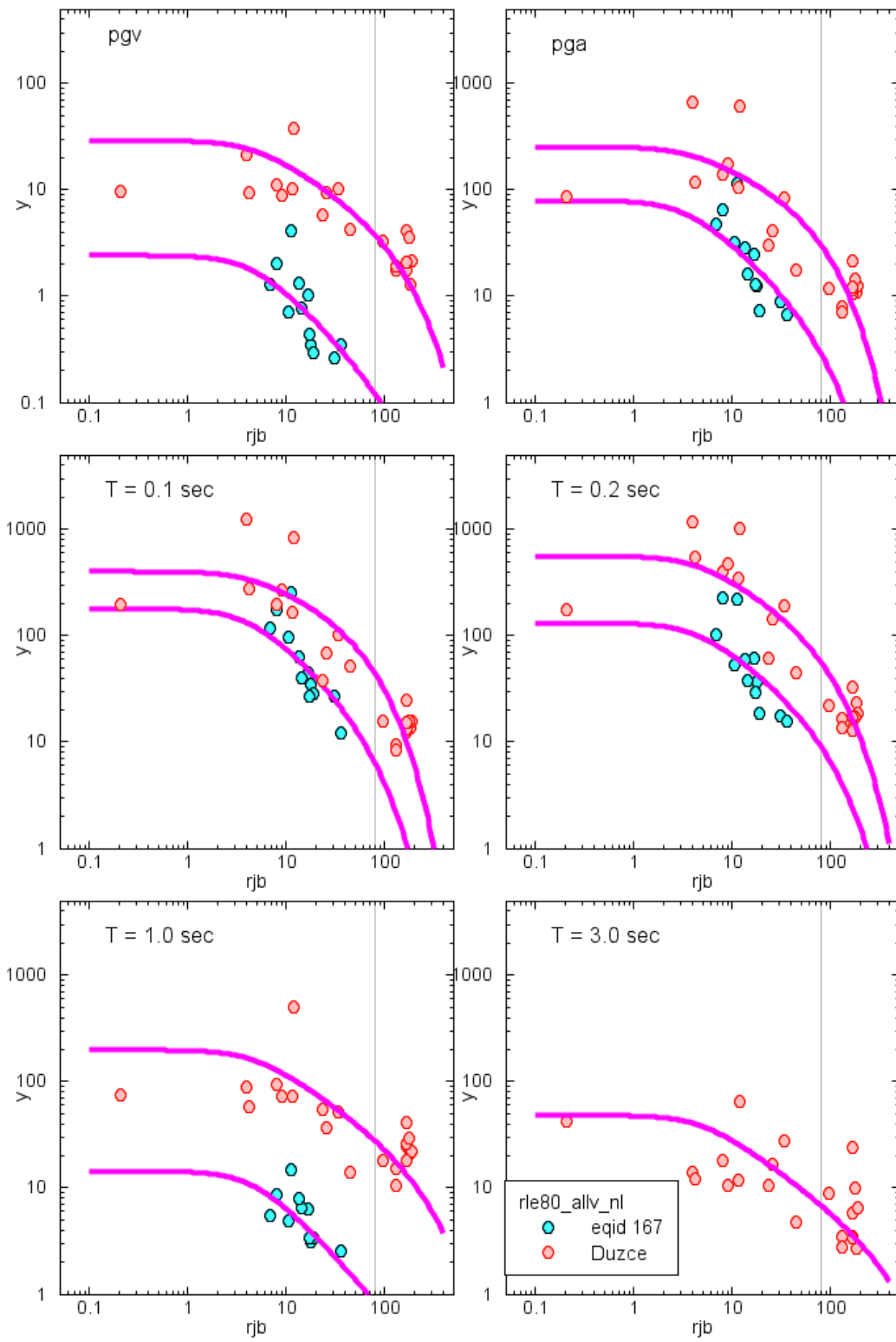
File: C:\peer_ngatteam\stage1_gm_rle80_allv_nl_eqid_137_167.draw; Date: 2006-12-07; Time: 10:58:55



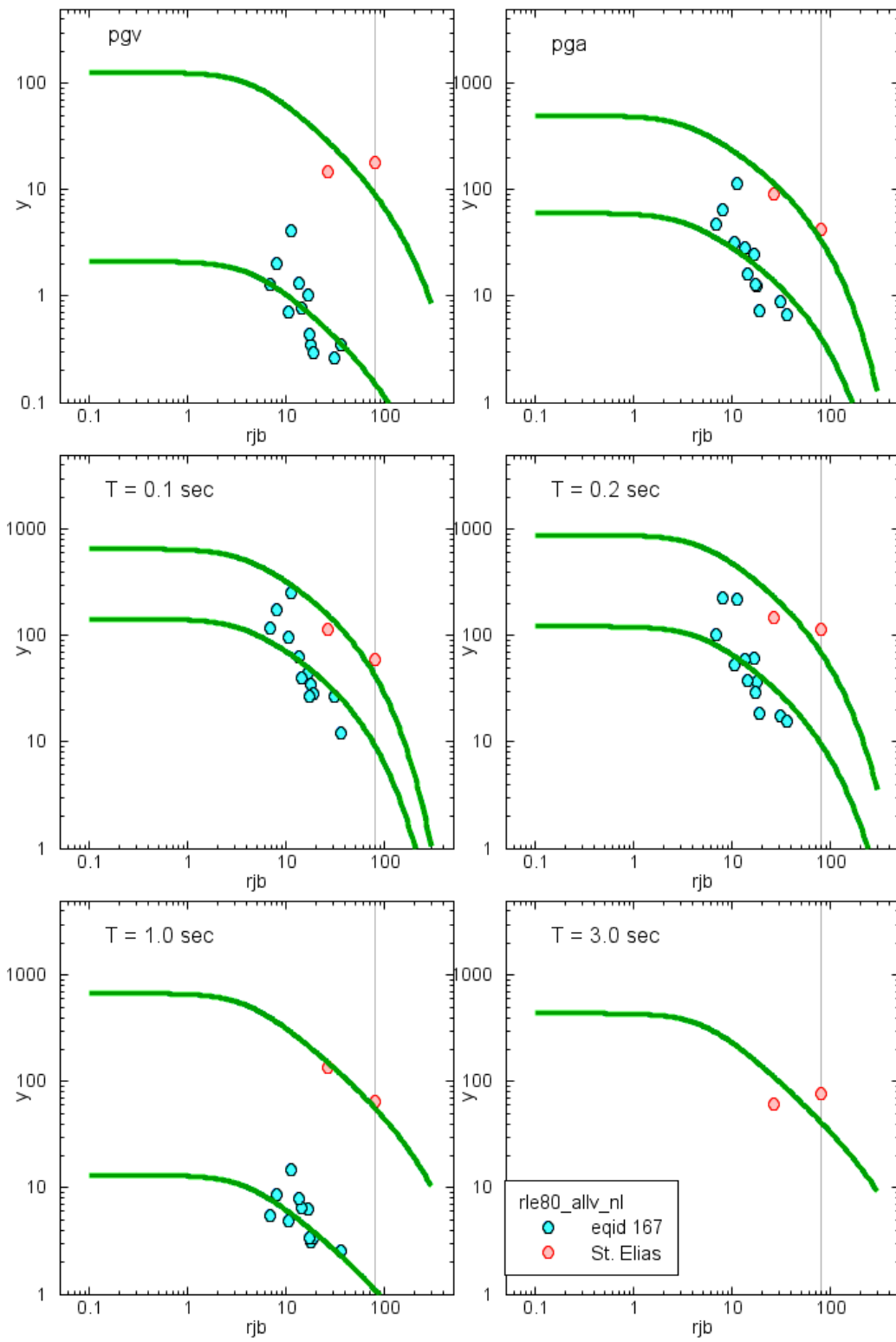
File: C:\peer_ngatteam\stage1_gm_rle400_o1_o2_fix_h_allv_nl_eqid_137_167.draw; Date: 2005-12-12; Time: 17:45:10



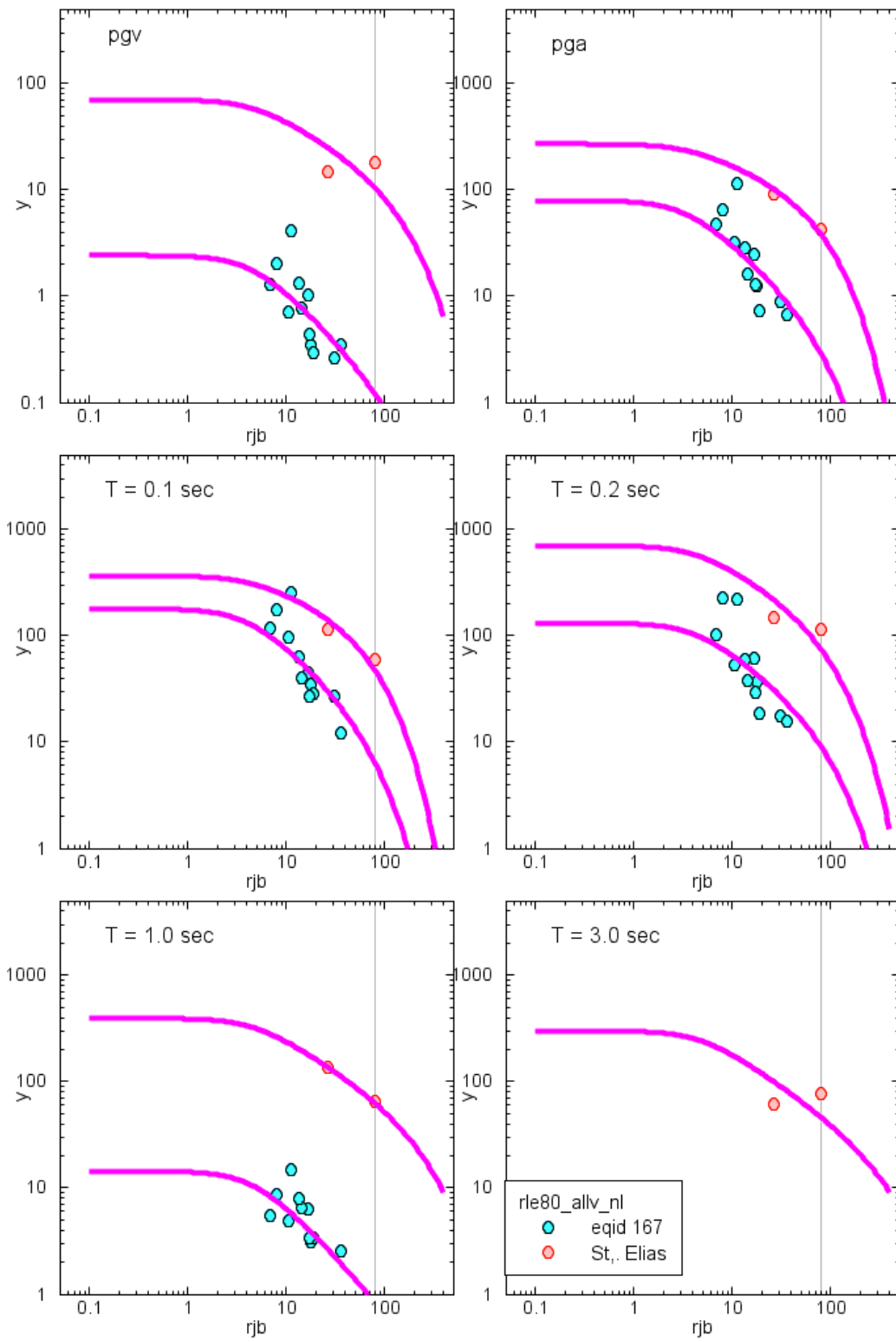
File: C:\peer_ngatteam\stage1_gm_rle80_allv_nl_eqid_167.dwg; Date: 2006-12-07; Time: 10:54:42



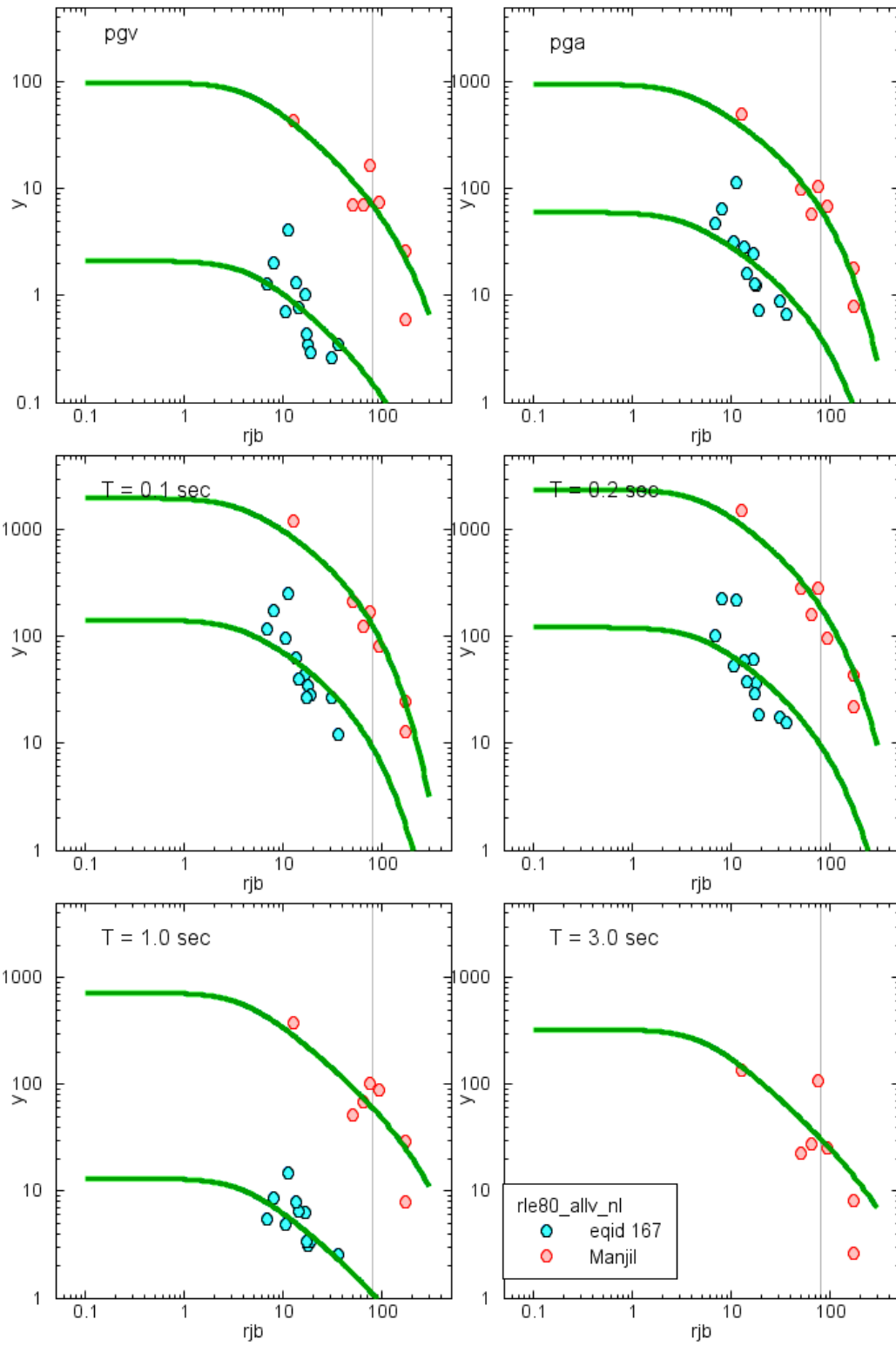
File: C:\peer_ngeteam\stage1_gm_tle400_o1_o2_fix_h_allv_nl_eqid_138_167.draw; Date: 2005-12-12; Time: 17:46:02



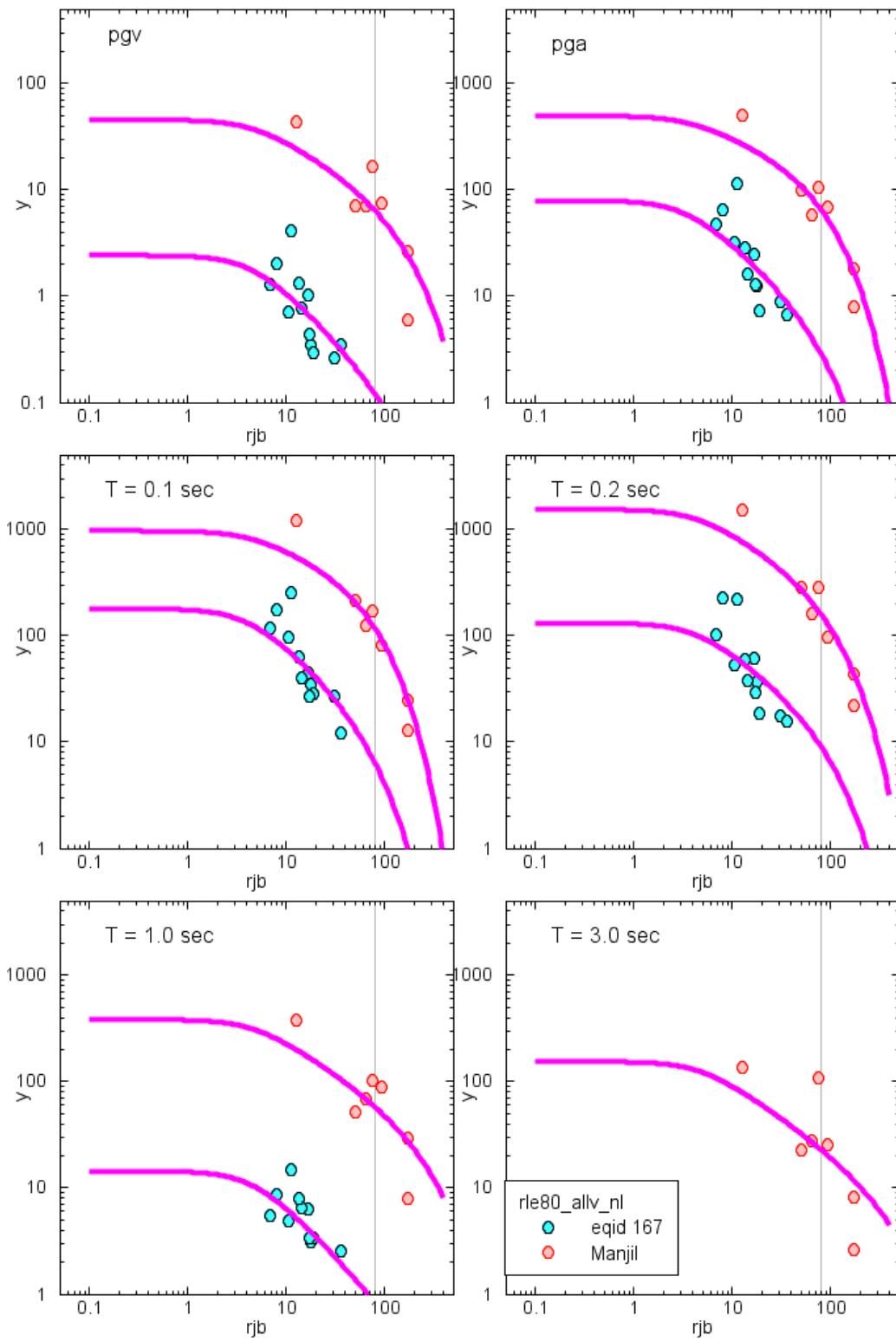
File: C:\peer_ngatteam\stage1_gm_rle80_allv_nl_eqid_142_167.draw; Date: 2006-12-07; Time: 10:58:01



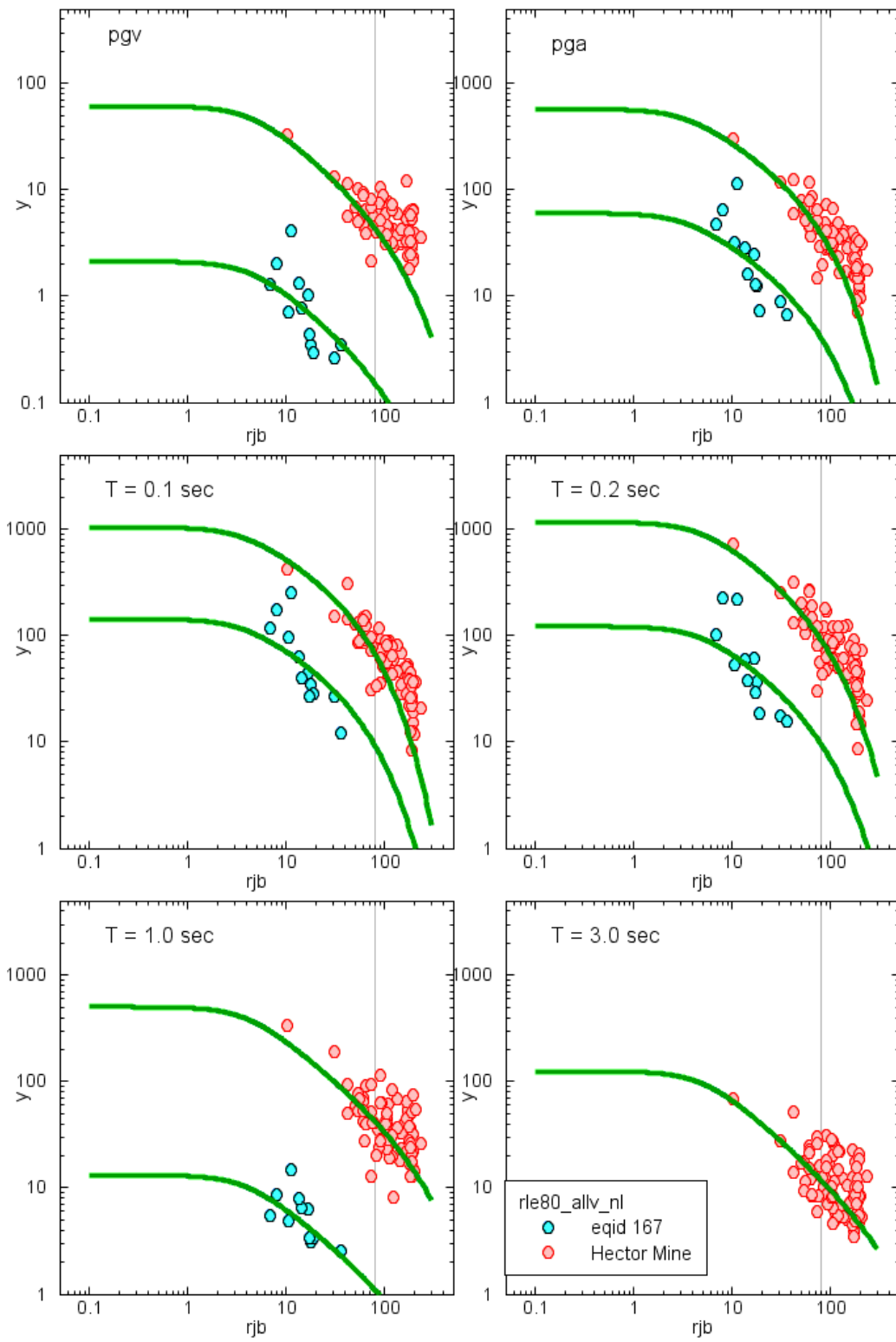
File: C:\peer_ngeteam\stage1_gm_rle400_e1_e2_fix_h_allv_nl_eqid_142_167.draw; Date: 2005-12-12; Time: 17:46:50



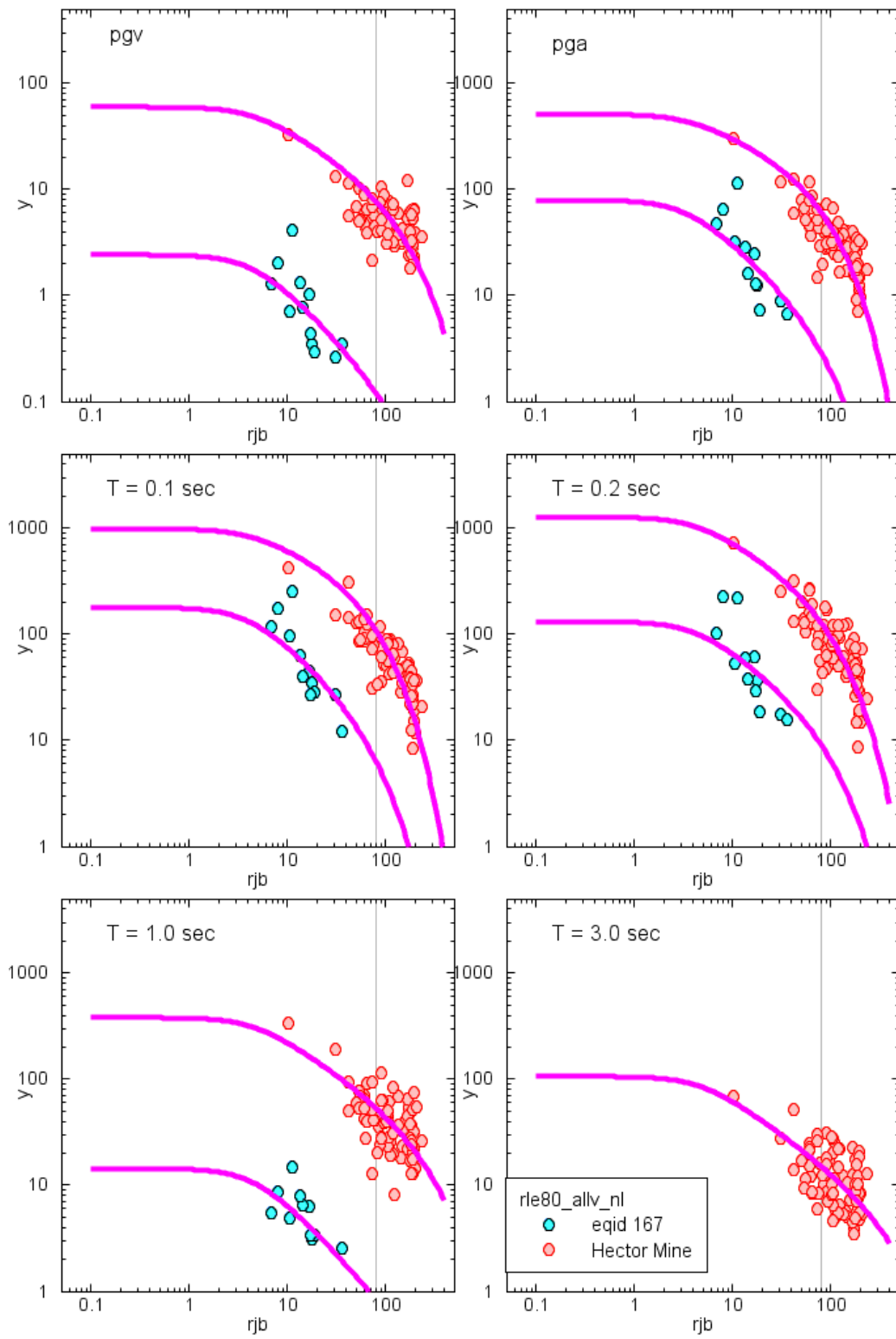
File: C:\peer_ngeam\stage1_gm_rle80_allv_nl_eqid_144_167.draw; Date: 2006-12-07; Time: 19:56:21



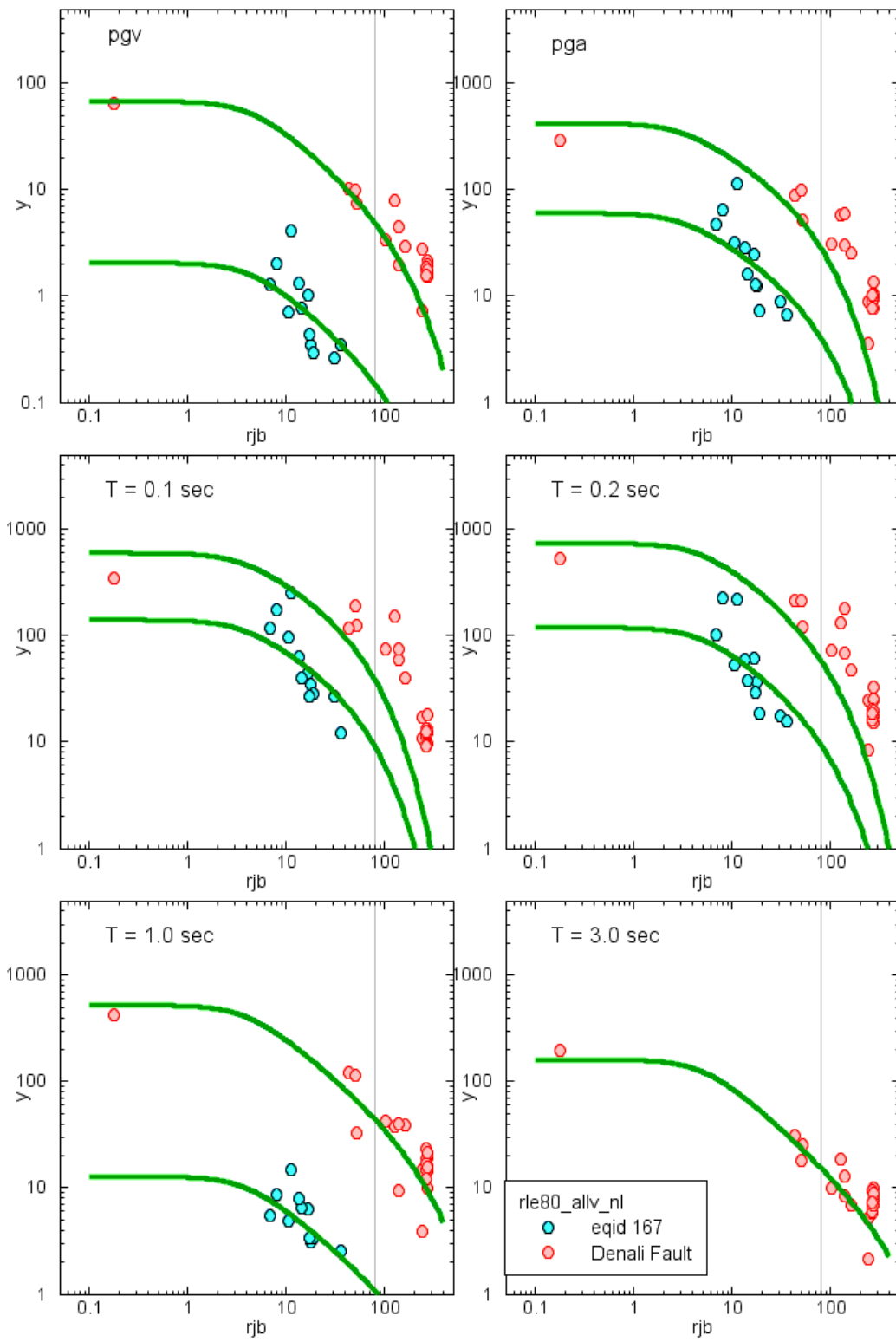
File: C:\peer_ngatteam\stage1_gm_tle400_e1_e2_fix_h_allv_nl_eqid_144_167.draw; Date: 2005-12-12; Time: 17:47:40



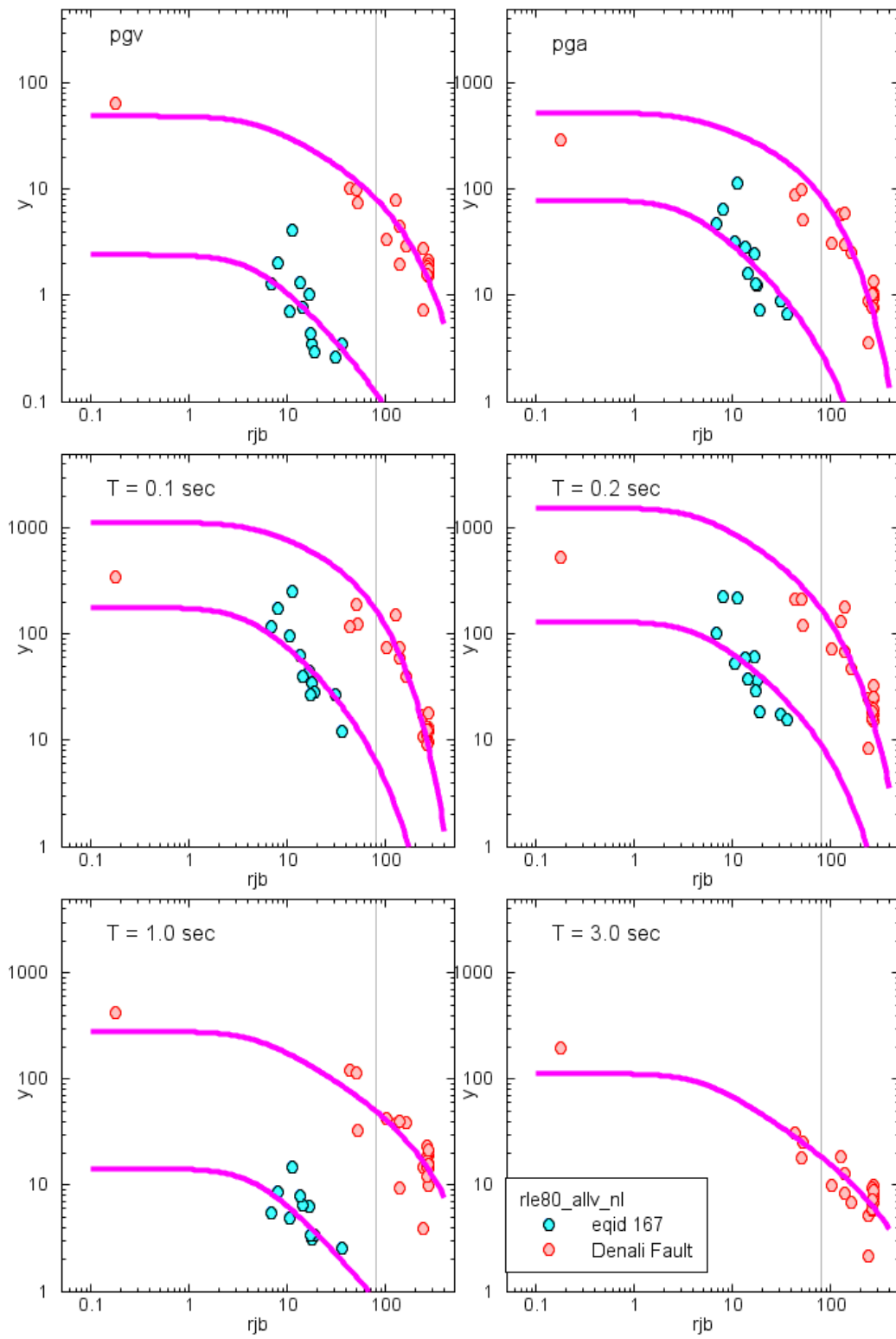
File: C:\peer_ngeatam\stage1_gm_rle80_allv_nl_eqid_167.draw; Date: 2006-12-07; Time: 10:53:40



File: C:\peer_ngatteam\stage1_gm_tle400_e1_e2_fix_h_allv_nl_eqid_167.draw; Date: 2005-12-12; Time: 17:48:48

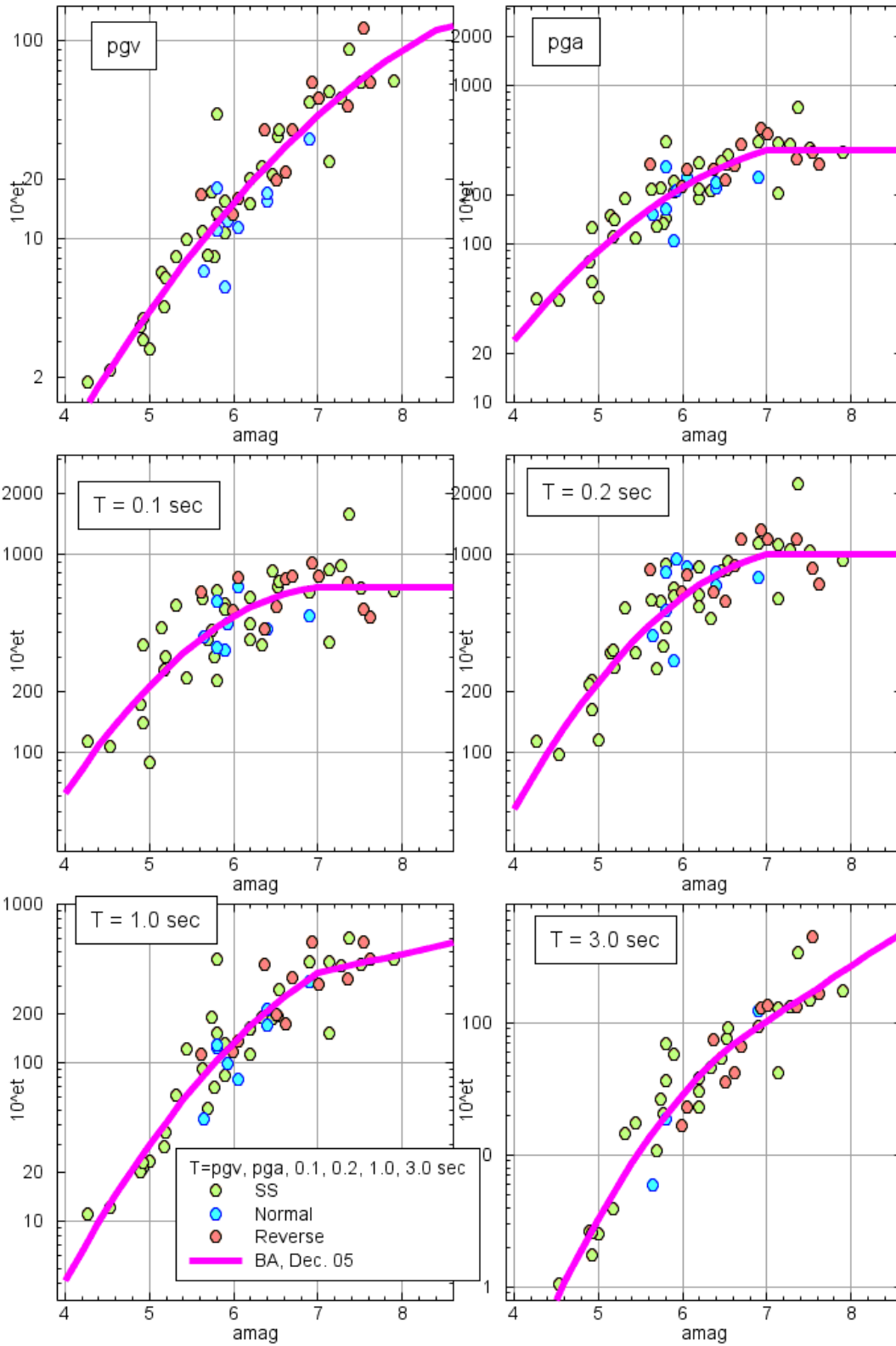


File: C:\peer_ngatteam\stage1_gm_rle80_allv_nl_eqid_167.draw; Date: 2005-12-12; Time: 15:38:18

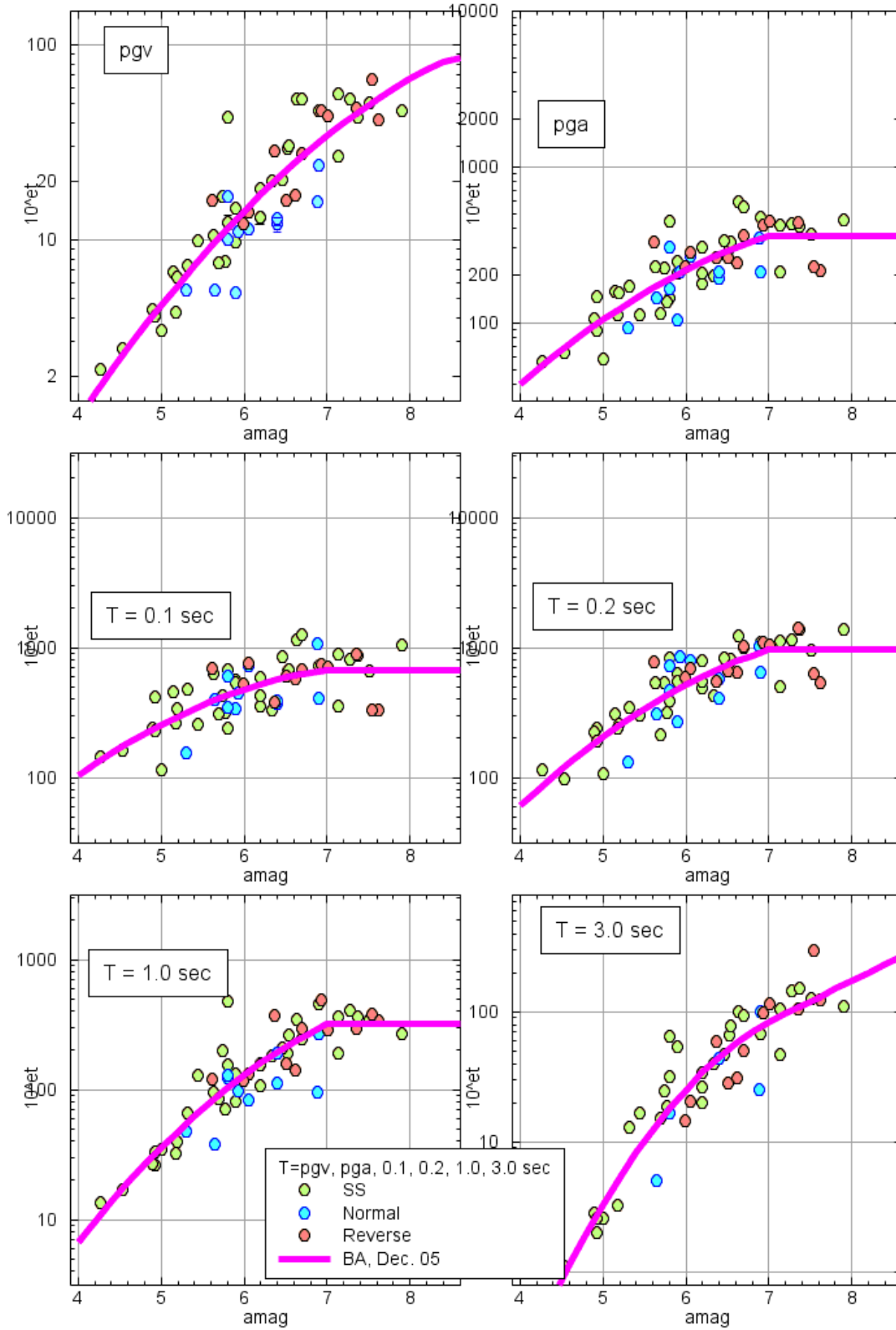


File: C:\peer_ngeatteam\stage1_gm_tle400_e1_e2_fix_h_allv_nl_eqid_167.draw; Date: 2005-12-12; Time: 17:40:39

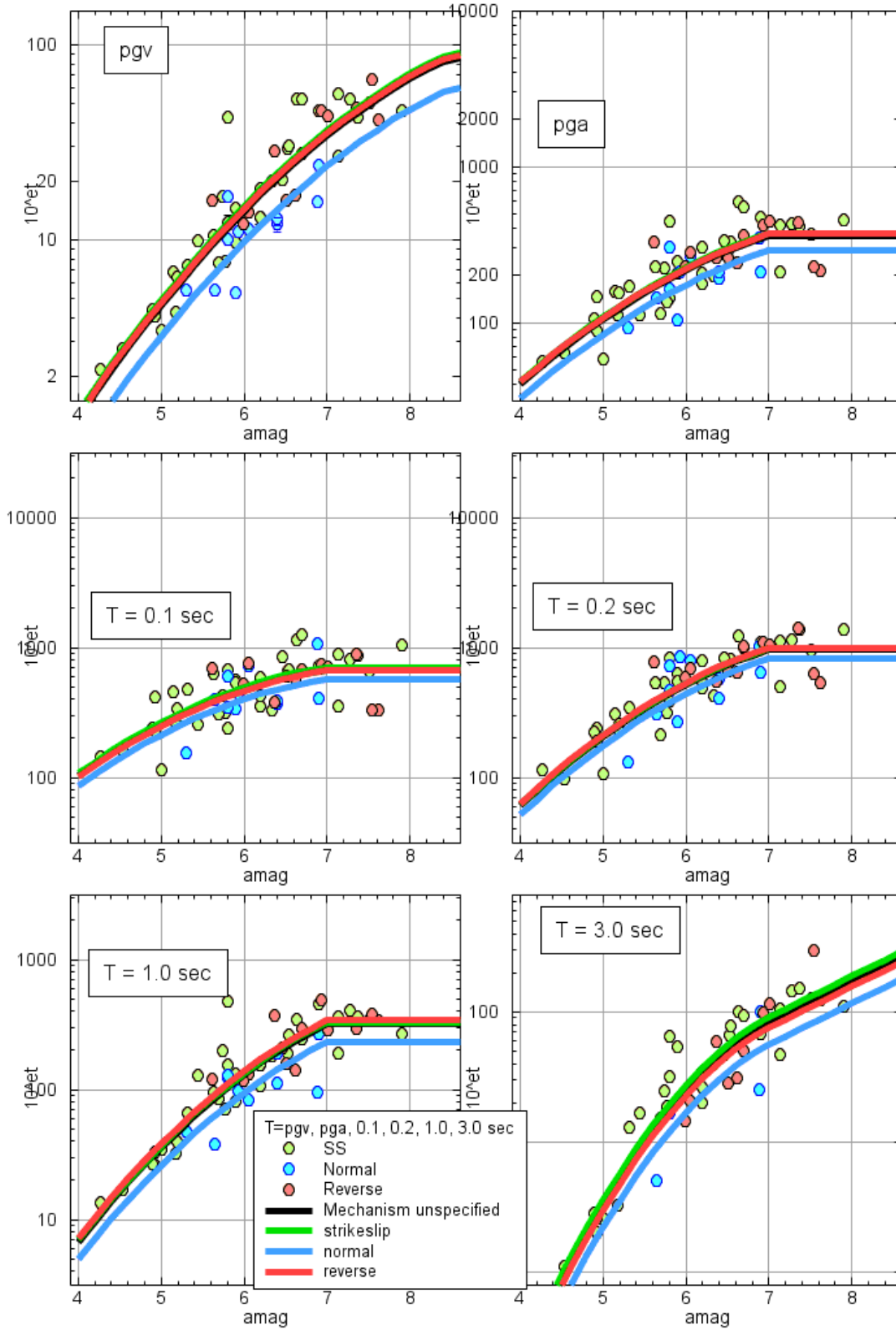
Here are plots of the event terms as a function of magnitude, with the regression curve superimposed. The first plot corresponds to the equivalent of the August equations. The second and third plots correspond to the equations in this report with mechanism unspecified and divided into strikeslip, normal, and reverse faults (the type of mechanism for each earthquake is indicated by the symbol color).



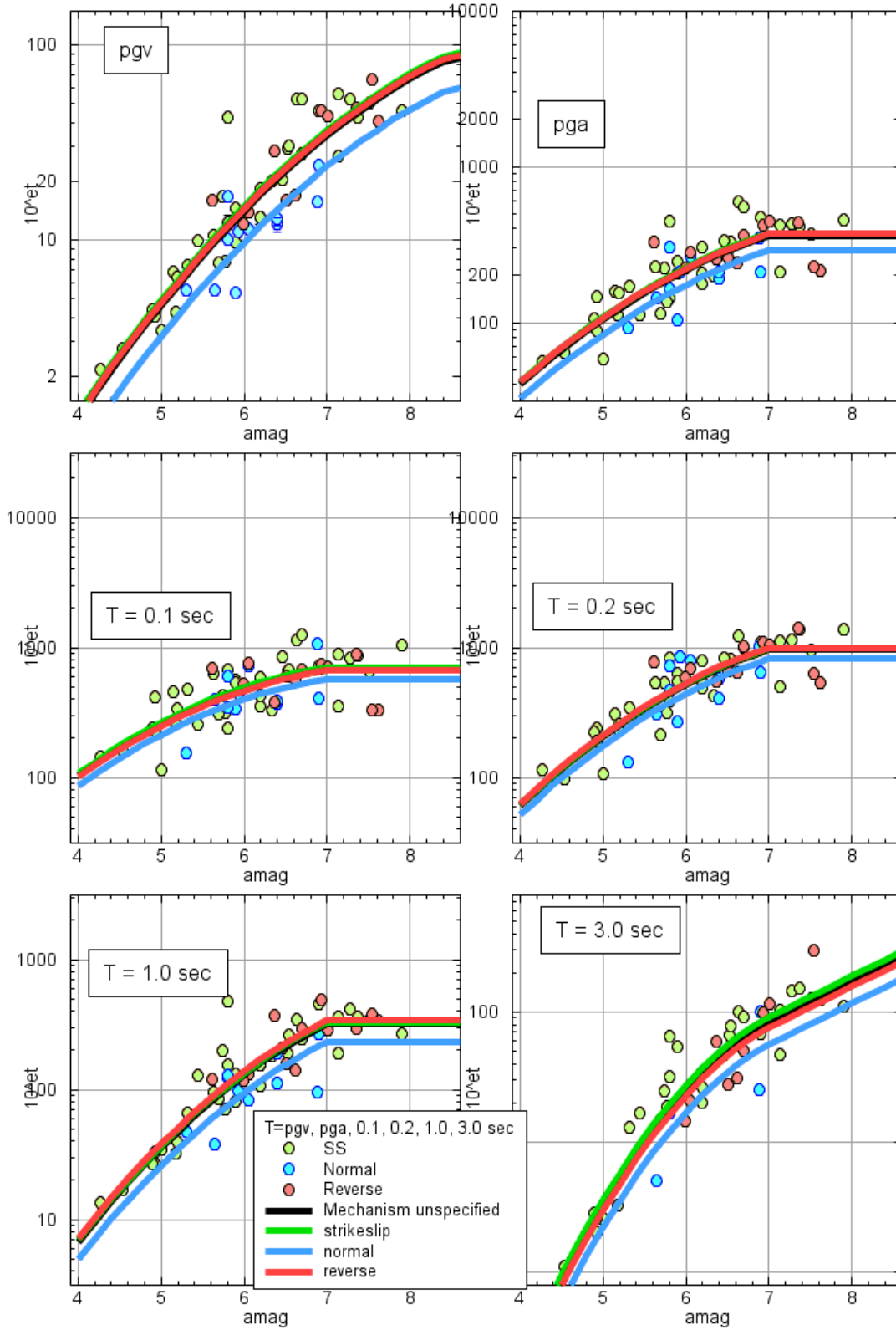
File: C:\peer_ngeteamxls1_et_ile80_allv_nl_vs_m_draw; Date: 2005-12-12; Time: 17:23:50



File: C:\peer_nrgalteam\st1_et_ile400_c1_c2_fix_h_alliv_nl_vs_m_draw; Date: 2005-12-12; Time: 17:30:40



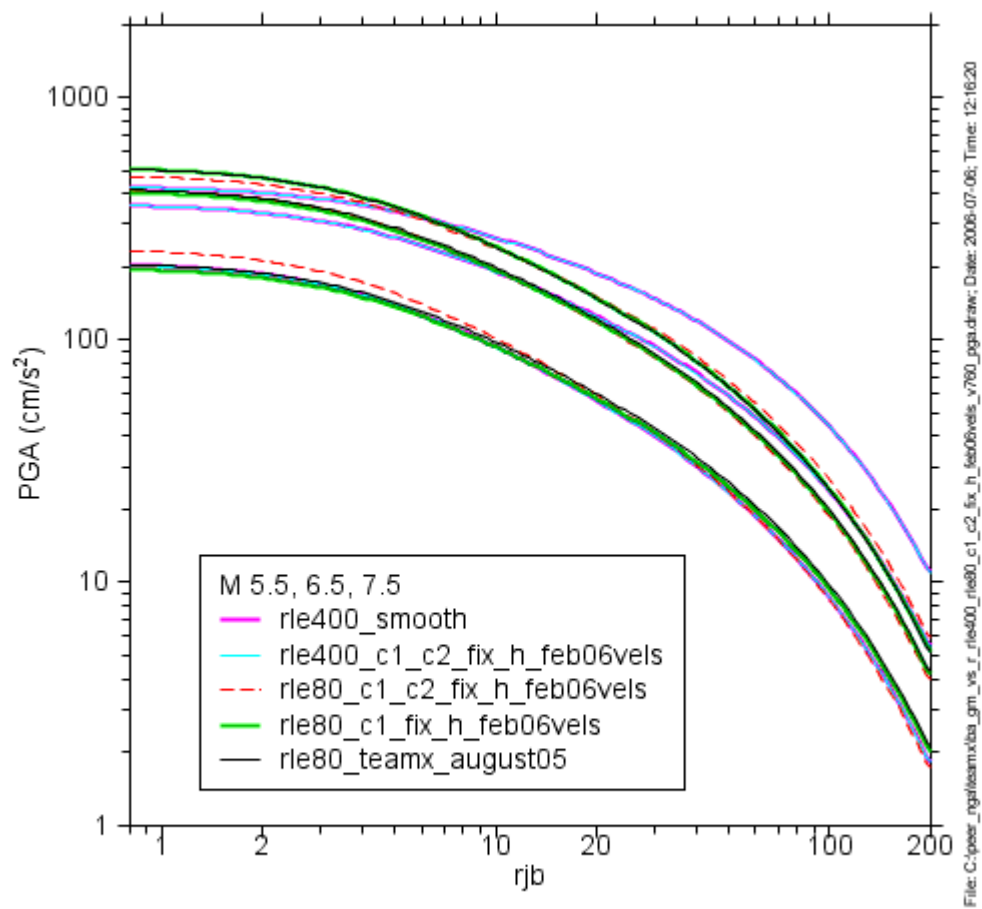
File: C:\peer_ngalteam\k1_et_le400_c1_c2_fix_h_allv_n1_mech_vs_m_draw Date: 2005-12-13; Time: 12:36:32

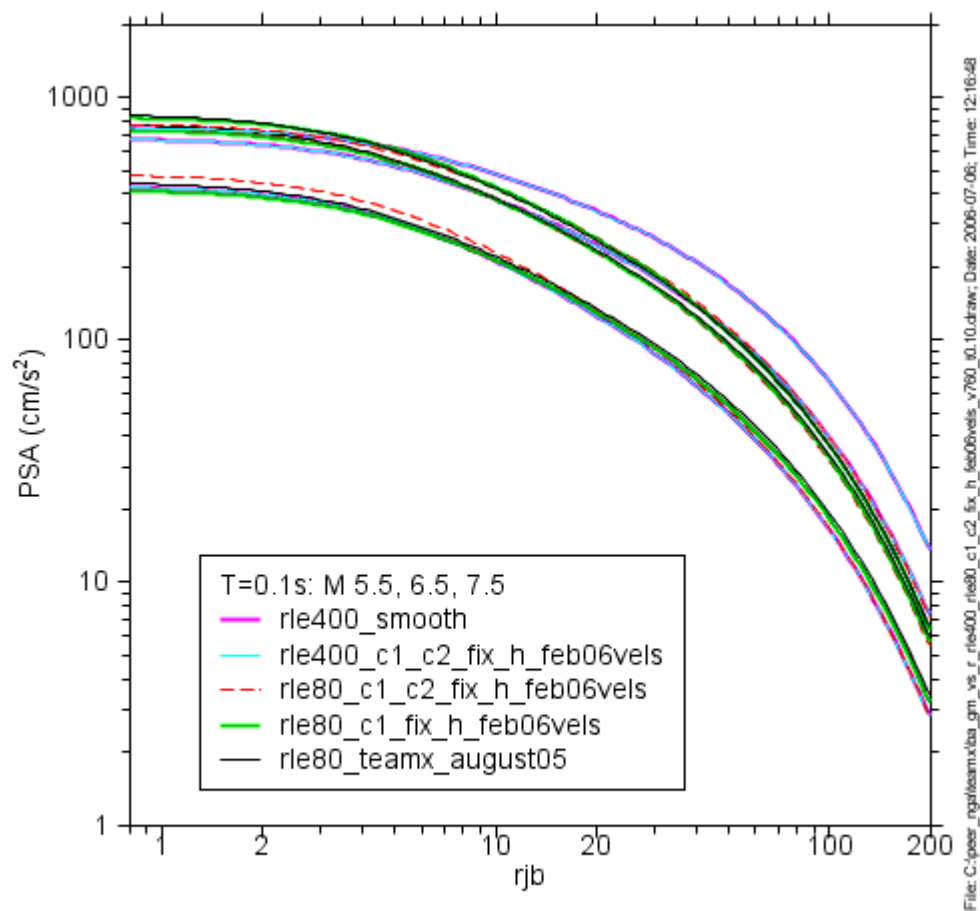


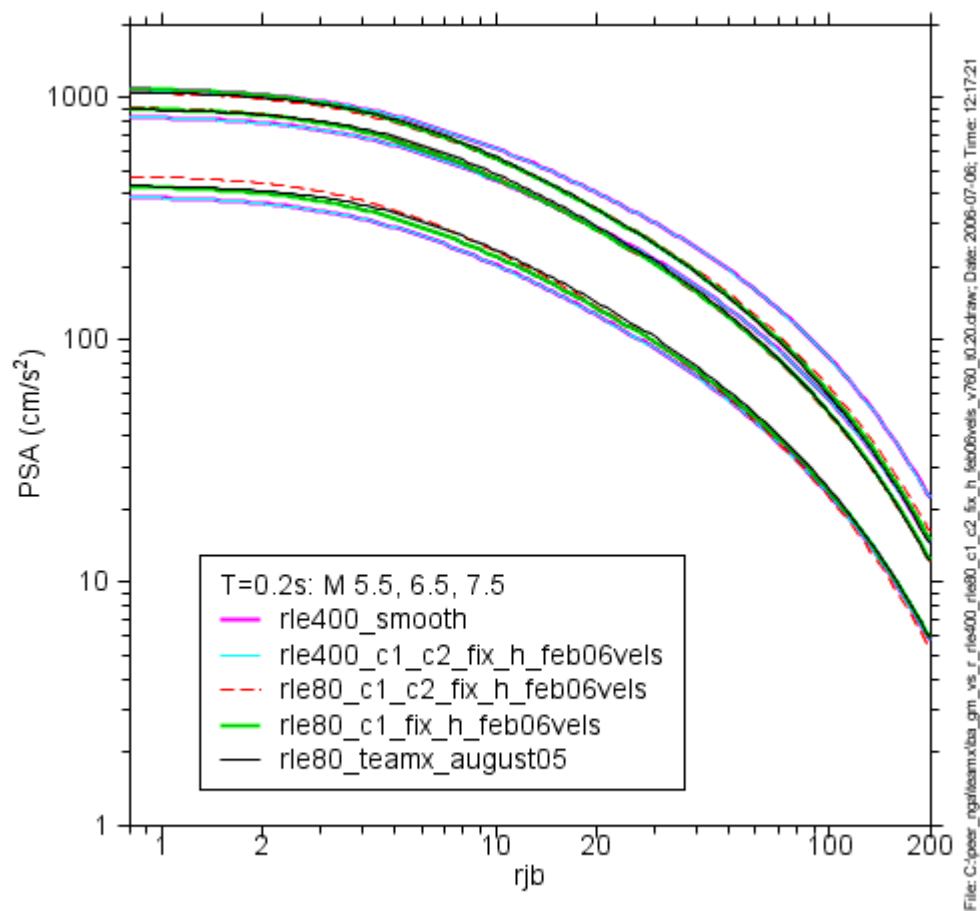
File: C:\peer_ngateam\sl1_et_tle400_c1_c2_fix_h_feb06vels_mech_vs_m.draw; Date: 2006-03-09; Time: 12:29:07

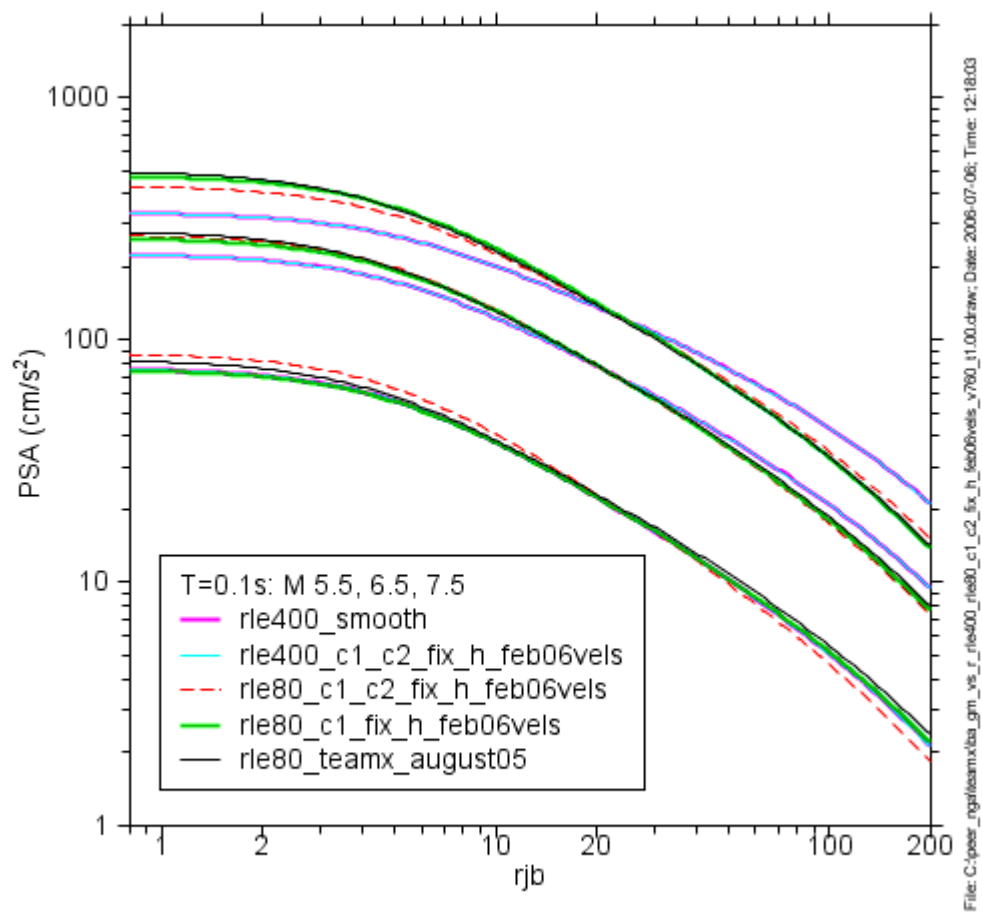
Comparison with BJJ Predictions

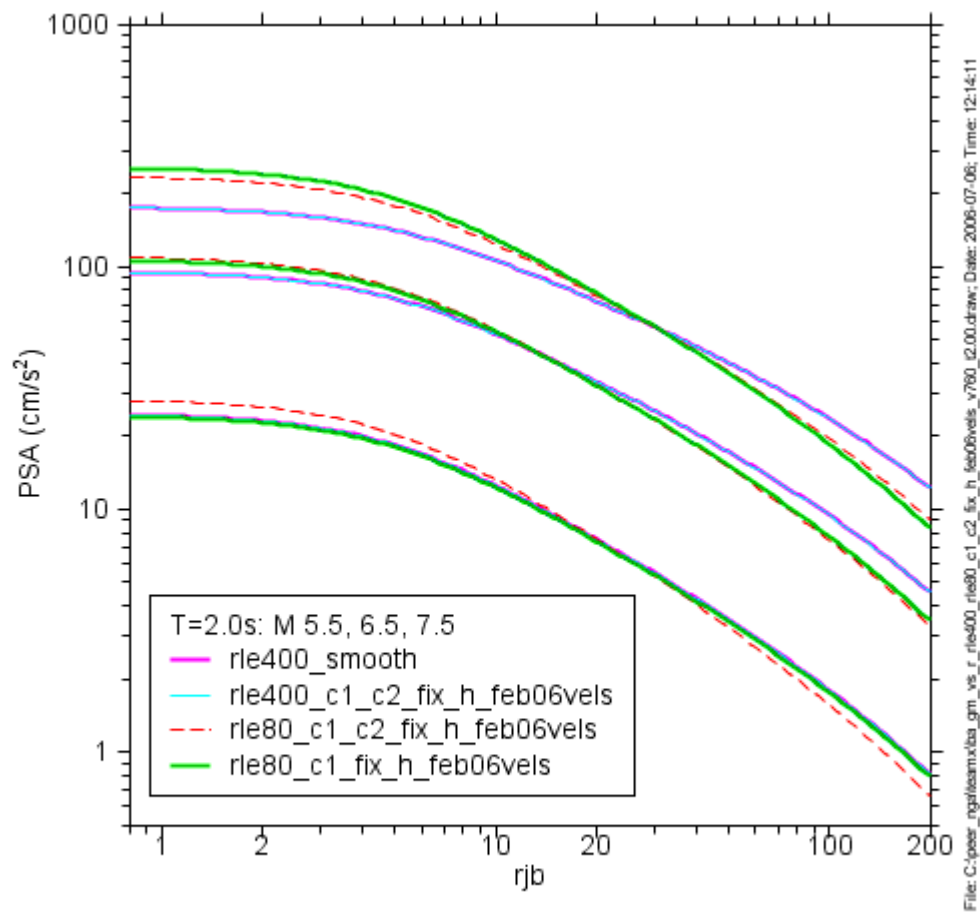
Below we show a comparison of ground motion predictions for the BJJ equations, the updated version of the August equations (rle80_c1_free_h), the equations from the May 31, 2006 version of this report, and the latest equations that include smoothing of the nonlinear amplification in the vicinity of $pga_{4nl} = 0.06g$ (rle400_c1_c2_fix_h_feb06vels_smooth). The motions are for an unspecified mechanism and $V_{30} = 760$ m/s. Curves are shown vs. distance for magnitudes of 5.5, 6.5, and 7.5. Plots are given for pga and 0.1, 0.2, 1.0, 2.0, and 3.0s oscillators, and for pgv . As shown here, there is very little difference in ground-motion predictions from the May31 and the July 6 versions of the equations. This is not too surprising, because the motions are for $V_{30} = 760$ m/s, for which there is no nonlinear amplification. Some idea of the difference in motions for a site with lower shear-wave velocity is given in the first figure in this report. There will be little difference in motions except for values of magnitude and distance for which pga_{4nl} is close to $0.06g$.

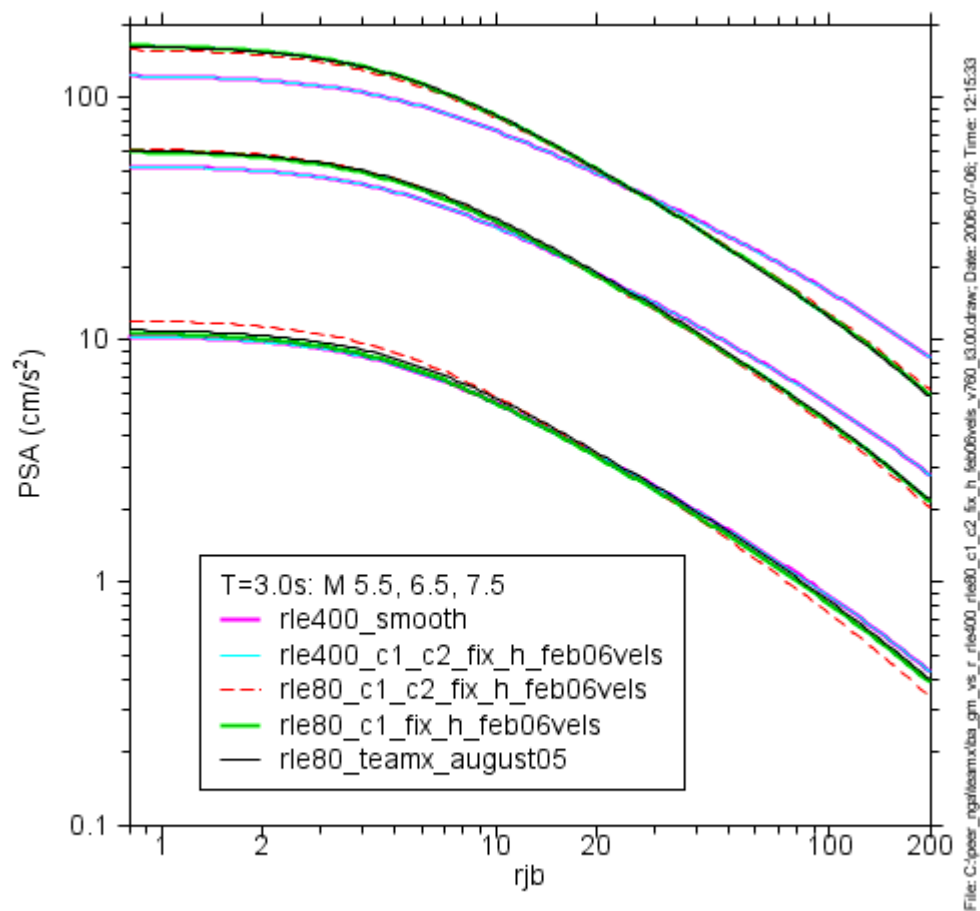


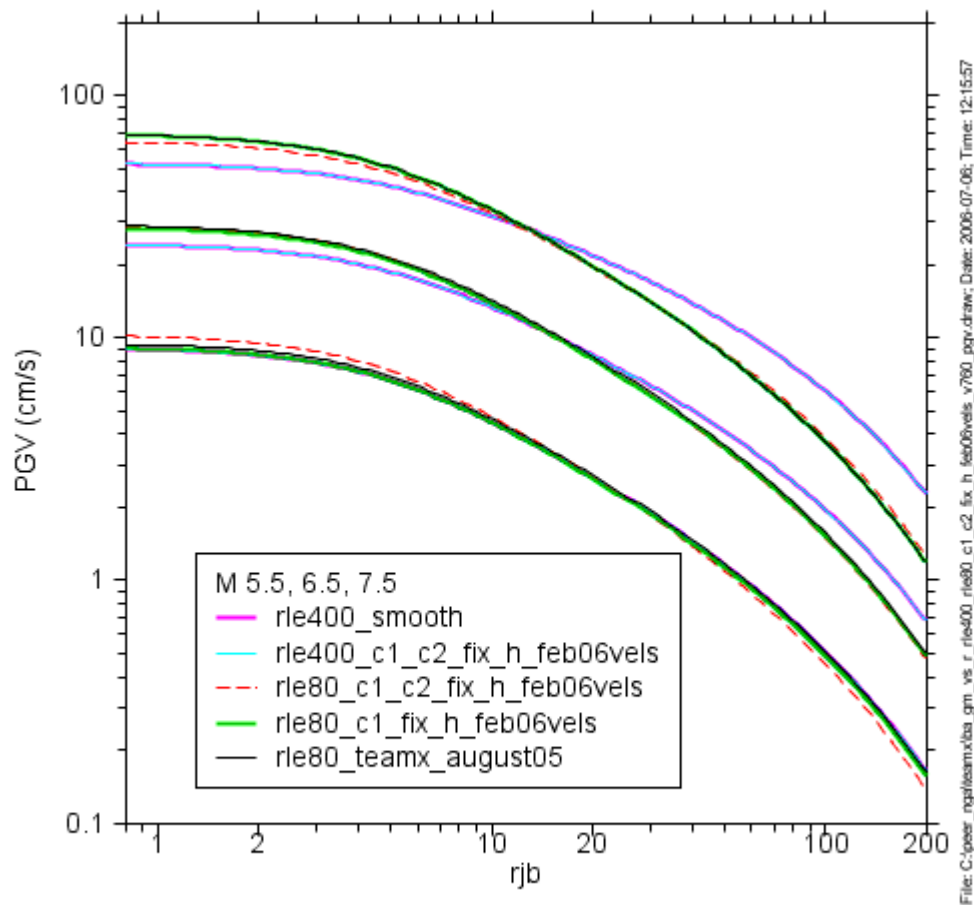












References

- Bommer, J. J. and J. E. Alarcón (2005). The prediction and use of peak ground velocity, *J. of Earthquake Engineering* **9**, (in press).
- Boore, D. M., W. B. Joyner, and T. E. Fumal (1993). Estimation of response spectra and peak accelerations from western North American earthquakes: An interim report, *U. S. Geological Survey Open-File Report* **93-509**, 72 pp.
- Boore, D. M., W. B. Joyner, and T. E. Fumal (1994). Estimation of response spectra and peak accelerations from western North American earthquakes: An interim report, Part 2, *U. S. Geological Survey Open-File Report* **94-127**, 40 pp.
- Boore, D. M., W. B. Joyner, and T. E. Fumal (1997). Equations for estimating horizontal response spectra and peak acceleration from

western North American earthquakes: A summary of recent work, *Seism. Research Letters* **68**, 128—153.

Boore, D. M., J. Watson-Lamprey, and N. A. Abrahamson (2006). GMRotD and GMRotI: Orientation-independent measures of ground motion, *Bull. Seism. Soc. Am.* **96**, (in press), available from <http://quake.usgs.gov/~boore>}

Choi, Y. and J. P. Stewart (2005). Nonlinear site amplification as function of 30 m shear wave velocity, *Earthquake Spectra* **21**, 1—30.

Joyner, W.B. and D.M. Boore (1993). Methods for regression analysis of strong-motion data, , *Bull. Seism. Soc. Am.* **83**, 469—487.

Joyner, W. B. and D. M. Boore (1994). Errata, , *Bull. Seism. Soc. Am.* **84**, 955—956.